

RESILIENT PROPERTIES OF UNSATURATED BASE MATERIALS

BY

RANJAN KUMAR ROUT

Presented to the Faculty of the Graduate School

of

The University of Texas at Arlington

In Partial Fulfillment of the Requirements for the Degree of

MASTER OF SCIENCE IN CIVIL ENGINEERING

THE UNIVERSITY OF TEXAS AT ARLINGTON

May 2012

To My Family

ACKNOWLEDGEMENTS

I would like to convey my gratitude and appreciation to Dr. Anand J Puppala, my supervising professor, for his guidance and support given to me for my study at The University of Texas at Arlington. I am grateful for Dr. Laureano R. Hoyos, and Dr. Xinbao Yu, members of the supervising committee for their valuable time and suggestions. I would also like to express my sincere thanks to Dr. Bhaskar Chittoori (Sinu), Dr. Thornchaya Wejrungsikul (Pomme), and Dr. Claudia Liliana Velosa for their suggestions and support during my research. I also thank them for enhancing my knowledge of soil and soil mechanics.

I would like to thank the UTA staff, Ginny Bowers, Sarah Ridenour, Ava Chapman, and Paul Shover for their friendly nature and unconditional help during my study and also the National Cooperative Highway Research Program (NCHRP) for funding this research.

I would like to thank my friend, Pinit Ruttanapornmakul (Tom) for helping me with the continuous support throughout the research work. I would like to appreciate my friends and colleagues Dr. Ekarut Archeewa, Ahmed Gaily, Anil Kumar Raavi, Andres, Aravind Pedarla, Nagasreenivasu Talluri, Raja Veerendra Yenigalla, Rajini Kanth Reddy, Seema Kalla, Tejo Vikash, Ujwal Patil and Varagorn Pulijan (Gate) for helping me out with the research work. My special thanks to my friends Ashraf Syed, Charan Cherukuri, Hari Ganji, Harshan Ravi, Leena Kantheti, Nandan Vempati, Pavan Gabbita, Preethi Suriamoorthy, Rakesh

Raju Doriaswamy, Ramya Kantheti, Venkateswararao kondepi, and Vishnu Paturi for their unconditional support during my stay in United States.

I am grateful for the love and support given by my mother Basanthi Rout, my dad Banmali Rout, my sister Swapna Rout, and my brother Deepak kumar Rout.

April 11, 2012

ABSTRACT

RESILIENT PROPERTIES OF UNSATURATED BASE MATERIALS

Ranjan Kumar Rout, M.S

The University of Texas at Arlington

Supervising Professor: Anand J Puppala

A pavement system basically consists of a surface layer, a base course, a subbase (optional) and the subgrade. As per MEPDG and 1993 AASHTO flexible pavement design guide Resilient Modulus (M_R) is used as the primary input parameter to determine the stiffness parameters and the constitutive behavior of pavement components, such as subgrade and unbound bases. Generally, pavements are constructed on compacted soils that are typically unsaturated with degrees of saturation varying from 75 to 90%.

The main focus of this research is to determine the effect of matric suction on the resilient moduli property of the base materials. The second objective of the research is to study the use of MEPDG models to calibrate resilient moduli properties either as a function of moisture content or soil suction variables. In

order to assess these objectives, these unbound materials were tested using suction controlled M_R and moisture controlled M_R procedures. Amendments were done by preparing the specimens at five different moisture content and dry density conditions. Suction controlled M_R testing took longer time to reach the equilibrium conditions and the results obtained were close to the results obtained from moisture controlled M_R procedure.

The initial suction conditions are studied using Fredlund device (Tempe cell). Test results indicate that the specimens compacted on the dry side of the optimum have high resilient modulus due to the stress hardening behavior. MEPDG program procedure was followed to predict the soil water characteristic curve. Lastly, two three model parameter models developed by Cary and Zapata (2010) and Modified Universal model are studied and analyzed in detail. Validity of the correlation equations are addressed by comparing measured M_R to predicted M_R values. Results suggest that the models used are well suited for predicting the resilient modulus and soil water characteristic curve of the two unbound base materials

TABLE OF CONTENTS

| | |
|--|------|
| ACKNOWLEDGEMENTS | iii |
| ABSTRACT | v |
| LIST OF FIGURES | viii |
| LIST OF TABLES..... | x |
| Chapter | Page |
| 1. INTRODUCTION | 1 |
| 1.1 Overview..... | 1 |
| 1.2 Research Objectives | 2 |
| 1.3 Organization and Summary | 3 |
| 2. LITERATURE REVIEW | 5 |
| 2.1 Introduction..... | 5 |
| 2.2 Resilient Modulus | 5 |
| 2.3 Estimation of Resilient Modulus..... | 8 |
| 2.4 Factors Impacting Resilient Modulus of Compacted Geomaterials | 18 |
| 2.5 Summary | 33 |
| 3. EXPERIMENTAL PROGRAM..... | 34 |
| 3.1 Introduction..... | 34 |
| 3.2 Basic Soil Tests | 52 |

| | |
|---|-----|
| 3.3 Advanced Soil Tests..... | 39 |
| 3.4 Equipment Employed for the Resilient Modulus Testing | 51 |
| 3.5 Summary | 57 |
| 4. ANALYSIS OF STRENGTH AND RESILIENT MODULUS TEST RESULTS | 58 |
| 4.1 Introduction..... | 58 |
| 4.2 Unconfined Compressive Strength | 59 |
| 4.3 Soil Water Characteristic Curve (SWCC) Studies | 61 |
| 4.4 Resilient Modulus Test Results | 64 |
| 4.5 Modeling Analysis..... | 75 |
| 4.6 Summary | 89 |
| 5. SUMMARY AND CONCLUSIONS..... | 90 |
| 5.1 Summary | 90 |
| 5.2 Recommendations for future research | 92 |
| REFERENCES | 94 |
| BIOGRAPHICAL INFORMATION | 104 |

LIST OF FIGURES

| Figure | Page |
|---|------|
| 2.1 Definition of resilient modulus (Puppala 2008)..... | 6 |
| 2.2 Definition of modulus (Nazarian et al. 1996)..... | 7 |
| 2.3 Stress level in a pavement (Hopkins et al. 2007)..... | 19 |
| 2.4 Resilient moduli at different saturation conditions | 23 |
| 2.5 Effect of matric suction on resilient modulus (Edil et al. 2006)..... | 26 |
| 2.6 Resilient moduli prepared at different densities (Pacheco and Nazarian 2010) | 28 |
| 3.1 Grain Size Distribution | 37 |
| 3.2 Compaction Curve | 39 |
| 3.3 Sample Preparation Points for SWCC | 40 |
| 3.4 Saturation of a Sample | 42 |
| 3.5 (a) Tempecell setup used in this research (b) Saturation process of HAE Disk | 44 |
| 3.6 Triaxial Equipment | 45 |
| 3.7 Unsaturated Resilient Modulus Testing Equipment | 49 |
| 3.8 The Loading Frame and Triaxial Cell..... | 52 |
| 3.9 The Pneumatic System..... | 53 |
| 3.10 The Control and Data Acquisition System | 55 |
| 3.11 External LVDTs Assembly | 56 |
| 3.12 Software window showing the test data | 57 |

| | |
|--|----|
| 4.1 Unconfined Compressive Strength Results of El Paso specimens | 60 |
| 4.2 Unconfined Compressive Strength Results of Austin specimens..... | 61 |
| 4.3 SWCC of El Paso specimens..... | 63 |
| 4.4 SWCC of Austin specimens..... | 63 |
| 4.5 a) Saturating the specimen b) Specimen placed on the bottom pedestal c) Unsaturated equipment used in the study | 66 |
| 4.6 Suction Controlled M_R results of El Paso (OMC) specimen | 67 |
| 4.7 Comparison between M_R results from 1st and 2nd approach | 69 |
| 4.8 Variation of resilient modulus (M_R) of El Paso specimens compacted at (a) OMC-2%, and (b) OMC-1% | 70 |
| 4.9 Variation of resilient modulus (M_R) of El Paso specimens compacted at (a) OMC, and (b) OMC+1%..... | 71 |
| 4.10 Variation of resilient modulus (M_R) of Austin specimens compacted at (a) OMC-2%, and (b) OMC-1%..... | 72 |
| 4.11 Variation of resilient modulus (M_R) of Austin specimens compacted at (a) OMC%, and (b) OMC+1%..... | 73 |
| 4.12 Variation of resilient modulus (M_R) of Austin specimens compacted at OMC+2%..... | 74 |
| 4.13 Predicted vs Measured SWCC (a) El Paso (b) Austin | 78 |
| 4.14 M_R - Matric Suction relationship | 82 |
| 4.15 Predicted vs Measured M_R results (Universal model) | 83 |
| 4.16 Predicted vs Measured M_R results (Cary and Zapata model) (a) El Paso specimens and (b) Austin specimens..... | 88 |

LIST OF TABLES

| Table | Page |
|---|------|
| 2.1 Summary of correlations to estimate material properties | 16 |
| 2.2 Resilient moduli recommended by the MEPDG based on the soil classification..... | 17 |
| 2.3 Assessment of Approaches in Estimating Moduli of Compacted Geomaterials (Puppala, 2008)..... | 18 |
| 2.4 Parameters Relating Modulus to Index Properties of Geomaterials..... | 30 |
| 3.1 Sieve Analysis..... | 36 |
| 3.2 Basic Soil Properties..... | 36 |
| 3.3 Compaction Parameters | 38 |
| 3.4 Sample Preparation Points for UCS and M_R Testing | 41 |
| 3.5 Resilient Modulus Testing Sequence..... | 47 |
| 3.6 Cell Pressure, Pore-Air Pressure for Suction Controlled M_R Testing | 50 |
| 4.1 UCS test results of El Paso base material | 59 |
| 4.2 UCS test results of Austin base material..... | 60 |
| 4.3 Regression coefficients of El Paso soil (Suction Controlled Testing)..... | 80 |
| 4.4 Regression coefficients of El Paso soil | 80 |
| 4.5 Regression coefficients of Austin soil..... | 81 |
| 4.6 Measured vs Predicted M_R results of El Paso specimens..... | 86 |
| 4.7 Measured vs Predicted M_R results of Austin specimens | 87 |

CHAPTER 1

INTRODUCTION

1.1 Overview

A pavement could be defined as a hard surface constructed over the natural soil for the purpose of providing a stable, safe and smooth transportation medium for the vehicles. A pavement system basically consists of a surface layer, a base course, a subbase (optional) and the subgrade. The main function of the base is to spread the traffic loads sufficient to prevent over-stressing of the subgrade. To be effective, the base should possess considerably greater resistance to deformation than the subgrade. Therefore, the base course must have enough strength to carry loads without shear failure (Potturi 2006).

The new Mechanistic Empirical Pavement Design Guide and 1993 AASHTO flexible pavement design guide use Resilient Modulus (M_R) as the primary input parameter when characterizing subgrade and unbound bases. The performance of the pavement depends on many factors such as the structural adequacy, the properties of the materials used, traffic loading, climatic conditions and the construction method. Resilient modulus of soils is typically determined either by using different types of laboratory tests or using different methods of in situ nondestructive tests. This test measures the stiffness of cylindrical specimen that is subjected a cyclic or repeated axial load; it creates a relationship between

deformation and stresses in different materials and soil conditions, such as moisture and density.

Unsaturated soil behavior plays a significant role in the mechanical properties of compacted pavement materials. Pavements are constructed on compacted soils that are typically unsaturated with degrees of saturation varying from 75 to 90%. The soil suction due to the presence of water in soil particles has a significant effect on the pavement foundation stiffness and strength properties (MnDOT 2007 guidelines). Different types of models accounting for soil suction and water content properties have been proposed by many researchers for modeling the resilient modulus of soil and aggregates for several years. In this study, two models proposed by Cary and Zapata (2010) and Modified universal model are used. Both models are analyzed with respect to providing realistic resilient properties of the soils.

1.2 Research Objectives

The main objective of the research is to determine the effect of matric suction on the resilient moduli properties of an unbound base material. One of the unbound materials was tested using a suction controlled resilient modulus testing device. These results are compared with test results obtained from moisture controlled resilient modulus procedure. The second objective of this research is to study the use of MEPDG models to calibrate resilient moduli properties either as a function of moisture content or soil suction variables. To accomplish these objectives, the resilient moduli properties of unbound base

materials were tested using a repeated load triaxial test at different compaction conditions. The following tasks are performed to address the above research objectives.

- Review the available literature on aggregate bases, resilient modulus testing, and fundamental concepts of unsaturated soil mechanics.
- Examine the soil water characteristic curve at three different compaction related moisture content - dry density conditions using a Tempe cell (Fredlund SWCC device).
- Perform the resilient modulus testing using the repeated load triaxial test equipment on two base materials compacted at different moisture content levels that are related to different matric suction levels.
- Analyze the effects of suction and moisture content on resilient properties using a three parameter model.

All necessary index and moisture-density tests were carried out as per standard test methods. Resilient modulus testing was carried out as per AASHTO T-307 procedure.

1.3 Organization and Summary

A brief description of the content of each chapter included in the thesis is presented in the following paragraphs.

Chapter 2 presents an overview of literature review to cover the basic concepts of resilient modulus testing on unbound materials. In addition, the

review also presents different ways to estimate resilient modulus and the factors affecting resilient modulus.

Chapter 3 summarizes the basic properties of the base material. The experimental program, sample preparation, laboratory test equipment including unconfined compressive strength, repeated load triaxial test and, data acquisition procedure. Fundamentals of Tempe cell and the test procedures used to determine the Soil Water Characteristic Curve (SWCC) is given in detail.

Chapter 4 summarizes the results obtained from the advanced tests conducted on the base materials. Tests results from UCS, resilient modulus testing and SWCC are presented. The second part of this chapter provides the analysis performed on the test results obtained in this study. Measured and predicted values of resilient modulus and SWCC are compared.

Summary and conclusions derived from the test results, as well as some recommendations for future research are presented in Chapter 5.

List of references are included towards the end of the report supporting the current research.

CHAPTER 2

LITERATURE REVIEW

2.1 Introduction

This chapter covers the current literature review on resilient modulus testing on unsaturated soils. The main objective of this chapter was to present a brief review of resilient modulus (M_R) concept, followed by the different ways to estimate the M_R . The fundamental parameters that impact the resilient modulus of compacted geomaterials are presented.

2.2 Resilient Modulus

The resilient modulus testing provides a basic relationship between stress and deformation of pavement materials for the structural analysis of layered pavement systems. Resilient modulus is analogous to the elastic modulus used in elastic theories and is defined as a ratio of deviatoric stress to resilient or elastic strain experienced by the material under repeated loading conditions that simulate traffic loading.

Figure 2.1 presents a schematic of the resilient modulus parameter (M_R). During testing, the specimen is subjected to a dynamic cyclic stress and a static-confining stress provided by means of a triaxial pressure chamber. The static confining pressure simulates the lateral stresses caused by the overburden pressure and dynamic cyclic stress simulates the traffic wheel loading.

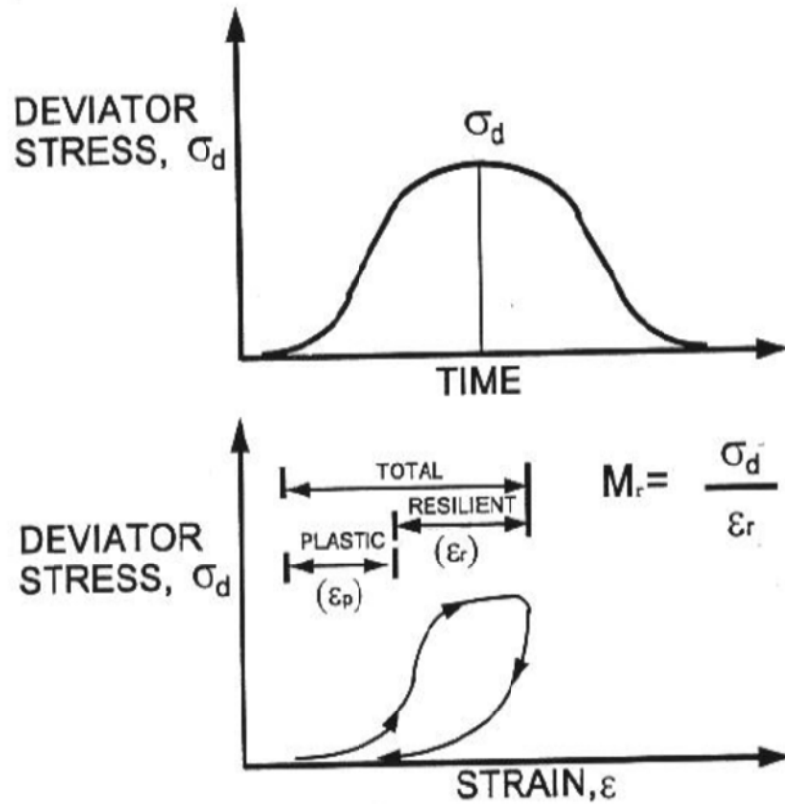


Figure 2.1 Definition of resilient modulus (Puppala 2008)

Loads applied on the soil specimens in the resilient modulus laboratory test are small when compared with ultimate loads of the same soils at failure. In the test method, the deformations measured during test cycles are considered as recoverable or elastic deformations and these recoverable deformations are used to estimate the resilient modulus parameter. Figure 2.2 presents other forms of moduli.

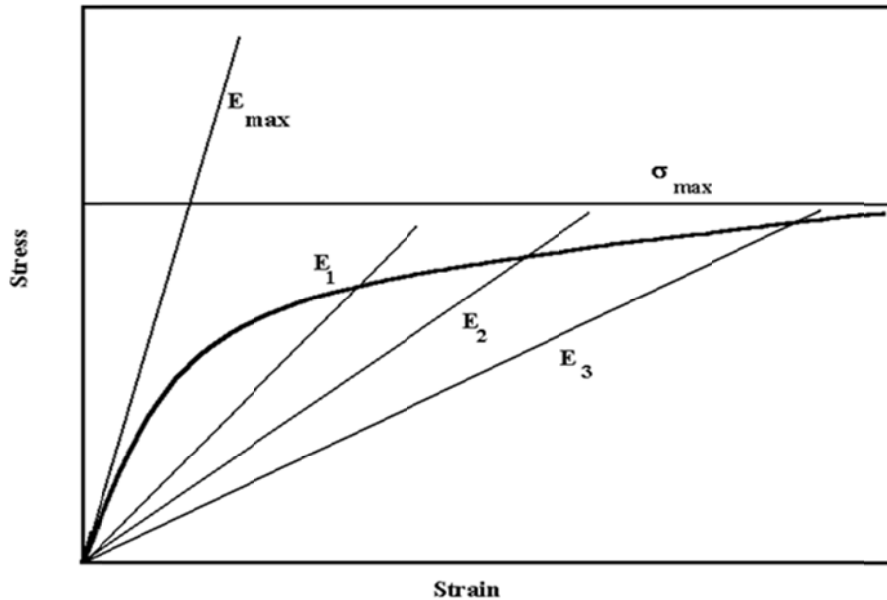


Figure 2.2 Definition of modulus (Nazarian et al. 1996)

Modulus is defined as ratio of the stress applied and measured strain. As reflected in the Figure 2.2 depending on the magnitude of the stress applied, the modulus can be an initial tangent modulus, E_{max} , or a secant modulus (E_1 through E_3). Resilient modulus is the modulus measured from repeated load testing and the importance of using resilient modulus as the parameter for subgrades and bases is that it represents a basic material property and can be used in the mechanistic analyses for indirectly predicting different distresses as rutting and pavement roughness.

As stated above, in laboratory testing, the soil specimens are subjected to a series of load pulses with distinct rest period, measuring the recoverable axial deformation and the applied load. Thus the resilient modulus is calculated as per the following expression:

$$M_R = \frac{\sigma_d}{\varepsilon_r} \quad (2-1)$$

Where σ_d is the axial deviatoric stress and is calculated from

$$\sigma_d = \frac{P}{A_i} \quad (2-2)$$

Where P is the applied load and A_i is the original cross-sectional area of the specimen. Parameter ε_r , the resilient strain, is calculated from

$$\varepsilon_r = \frac{\Delta L}{L_i} \quad (2-3)$$

Where ΔL is the recoverable axial deformation along a gauge length, L_i .

2.3 Determination of Resilient Modulus

The resilient modulus of a layer can either be measured with field or laboratory testing methods, or can be estimated based on empirical relationships or can be estimated based on soil property calibrations. A brief description of each of this method (termed as Levels in MEPDG) is provided in the following.

2.3.1 *Level 1-Laboratory or Field Testing*

2.3.1.1 Laboratory Testing

Laboratory tests are essential to study the parameters that affect the properties of materials. The behavior of a material in terms of variation in modulus with stress level, strain amplitude, and the strain rate is best established by conducting laboratory tests such as the resilient modulus test. However, resilient moduli from laboratory tests are moderately or significantly different than the in-situ test results. These differences can be due to sampling disturbance, differences in the state-of-stress between the specimen and in-place pavement

material, non-representative specimens, long-term time effects, and inherent errors in the field and laboratory test procedures (Anderson and Woods, 1975). A brief discussion of the laboratory tests to determine M_R properties is summarized below.

2.3.1.1.1 Repeated Load Triaxial Test

The Resilient Modulus test using RLT test equipment is designed to simulate traffic wheel loading on in situ subsoils by applying a sequence of repeated or cyclic loads on compacted soil specimens. The test procedure involves preparation of a compacted soil specimen using impact compaction or other methods, transfer of soil specimen into triaxial chamber, application of confining pressure, and then initiation of testing by applying various levels of deviatoric stresses as per the test sequence.

The test process requires both conditioning followed by actual testing under a multitude of confining pressure and deviatoric stresses. At each confining pressure and deviatoric stress, the resilient modulus value is determined by averaging the resilient deformation of the last five deviatoric loading cycles. Hence, from a single test on a compacted soil specimen, several resilient moduli values at different combinations of confining and deviatoric stresses are determined. RLT is most prominent method because this test is standardized by AASHTO and its features better simulation of traffic loading.

2.3.1.1.2 Other Laboratory Test

A hollow cylinder test simulates stress conditions close to the field traffic loading, including the principle stress rotations taking place in the subgrade caused by wheel load movements (Barksdale et al. 1997). In this test, a hollow cylindrical soil specimen is enclosed by a membrane both inside and outside the sample. Stresses are applied in axial or vertical, torsional, and radial directions. Repeated loads can be simulated in this setup and related moduli can be determined. Because of the possible application of various types of stresses, different stress path loadings simulating field loading conditions can be applied. Also, this setup can be used to perform permanent deformation tests.

Resonant column and Simple shear test are few other laboratory tests used to determine the resilient moduli. The principal advantage in using laboratory procedures to determine the resilient modulus is basically the capability of performing a controlled test. When performing a laboratory test; it is possible to control the confining pressure level as well as the shear stress level or both. On the other hand, laboratory procedures are time consuming and have a high cost which makes the procedure economically unsuitable for routine pavement design.

2.3.1.2 Field Tests

Several in situ methods have been used to predict or interpret the resilient moduli or stiffness of unbound materials and subgrades (pavement layers). Various test procedures and their methods for measuring resilient modulus

properties are described in the NCHRP synthesis by Puppala (2008). These methods are grouped into two categories: nondestructive methods and intrusive methods. In this section, few field methods are presented briefly.

2.3.1.2.1 Nondestructive Methods

Nondestructive methods for determining the stiffness (E) are based on several principles, including geophysical principles. Some of the methods involve the measurement of deflections of pavement sections subjected to impulse loads and then employ back-calculation routines to estimate the stiffness properties of pavement layers such that the predicted deflections match with the measured deflections.

2.3.1.2.1.1 Dynaflect

Dynaflect is a light-weight two-wheel trailer equipped with an automated data acquisition and control system. The pavement surface is loaded using two counter-rotating eccentric steel weights, which rotate at a constant frequency of eight cycles per second (8 Hz). This movement generates dynamic loads of approximately ± 500 lb (227 kg) in magnitude (Choubane and McNamara 2000). The total load applied to a pavement system is a combination of the static weight of the trailer and the dynamic loads generated by the rotating weights. The deflections of the pavement system are measured by five geophones suspended from the trailer and placed at 1 ft intervals. Deflection data monitored during the loading is then analyzed using both theoretical and empirical formulations to determine the modulus of subgrade and base layers.

2.3.1.2.1.2 Falling Weight Deflectometer (FWD)

FWD applies an impulse load on the pavement surface by dropping a weight mass from a specified height and then measures the corresponding deflections from a series of geophones placed over the pavement surface. Deflection profiles under different impulse loads will be measured and analyzed with different theoretical models of distinct constitutive behaviors to determine the modulus of various layers in the pavement system. The analysis uses backcalculation routines that assume a different modulus for each layer of the pavement and then use a specific algorithm to predict the deflections of the pavement surface. If the predicted deflection pattern and magnitudes match with the measured deflections, then the assumed moduli are reported as the moduli of the pavement layers.

2.3.1.2.1.3 Light Falling Weight or Portable Deflectometers

Among nondestructive assessment of pavement layers, portable deflectometer-type devices have been receiving considerable interest by several DOT agencies. Similar to the full-scale FWD-type tools, these devices utilize both dynamic force and velocity measurements by means of different modes such as transducers and accelerometers. These measurements are then converted to elastic stiffness of the base or subgrade system, which is equivalent to homogeneous Young's modulus of the granular base and subgrade layers, using equations that assume underlying layers as homogeneous elastic half-space. Factors that influence the stiffness estimation of field devices also influence

these methods, and hence some variations in moduli values are expected with the same group of devices that operate on different principles. A few of these Light Falling Weight or Portable Deflectometers used in the field are LFWD, LFD and PFWD.

2.3.1.2.2 Intrusive Methods

Intrusive or in situ penetration methods have been used for years to determine moduli properties of various pavement layers. Intrusive methods can be used for new pavement construction projects and also in pavement rehabilitation projects wherein the structural support of the pavement systems can be measured (Newcomb and Birgisson 1999). Few intrusive methods are briefly reviewed here

2.3.1.2.2.1 Dynamic Cone Penetrometer (DCP) Test

The DCP test is a widely used in situ method for determining the compaction density, strength, or stiffness of in situ soils. The DCP is a simple testing device, wherein a slender shaft is driven into the compacted subgrades and bases using a sliding hammer weight and the rate of penetration are measured. Penetration is carried out as the hammer drops to reach the desired depth. The rod is then extracted using a specially adapted jack. Data from the DCP test are then processed to produce a penetration index, which is simply the distance the cone penetrates at each drop of the sliding hammer. Typically, in this test, the measured soil parameter from the test is the number of blows for a given depth of penetration. Several parameters from DCP tests are typically

determined and these are termed as dynamic cone resistance (q_d) or DCP index (DCPI) in millimeters per blow or inches per blow or blows per 300 mm penetration. These parameters are used to evaluate the compaction density, strength, or stiffness of in situ soils.

2.3.1.2.2 Plate Load Test

Plate load tests (PLTs) were used for resilient moduli interpretations and a few states, including Florida and Louisiana, have attempted to use them for correlating with the resilient modulus of subgrades (Abu-Farskh et al. 2003). The PLT operations involve loading a circular plate that is in contact with the layer to be tested and measuring the deflections under load increments. Circular plates usually 30 cm (12 in.) in diameter are generally used and the loading is transmitted to the plates by a hydraulic jack.

During the test, a load- deformation curve will be recorded and these data will be used to estimate the moduli of the load-deformation or stress-strain plot, which is referred to as E_{PLT} . If the field test is performed in cyclic mode, then the slope of the stress–strain curve provides the moduli. The moduli measured from this test are regarded as composite moduli as the depth of influence is considered to extend more than one layer (Abu-Farsakh et al. 2003). Nelson et al. (2004) also reported the use of PLTs to estimate the moduli of compacted retaining wall backfill material. Though the PLT method is primarily used for rigid pavements, several researchers have attempted to correlate the moduli with the elastic moduli of the subgrades. More research is still needed to better

understand the applicability of this method in evaluating the resilient properties of subgrades and bases. Dilatometer, Pressuremeter, Static Cone Penetrometer are few other intrusive methods used in the field to determine the stiffness properties of the soils.

2.3.2 Level 2-Correlations with Other Material Properties

Due to the complexity and time-consuming nature of the resilient modulus laboratory tests, simple methods have been proposed for estimating the M_R of the geomaterials in the laboratory. It is also common to use strength tests, such as the unconfined compressive strength or laboratory based California Bearing ratio (CBR), to estimate the modulus property. However, if no resilient modulus test data is available, then the modulus value can be calculated using one of the empirical relationships presented in Table 2.1.

2.3.3 Level 3-Typical Values (Based on Calibration)

This level relies on the little or no testing information, sometimes mainly based on the material classification. Table 2.2 provides the determination of resilient moduli based on soil classification. These relationships, which are typically based on the index properties of geomaterials, can be used in design stages as the first approximation. Due to the general nature of these relationships and inherent variability in the geomaterials, the level of uncertainty in the estimated values is rather high.

Table 2.1 Summary of correlations to estimate material properties

| Strength/Index Property | Model | Comments | Test Standard |
|--------------------------|--|--|---|
| CBR | $M_r = 2555(CBR)^{0.64}$ | CBR=California Bearing Ratio, percent | AASHTO T 193-The California Bearing Ratio |
| R-value | $M_r = 1155 + 555R$ | R=R-value | AASHTO T190-Resistance R-Value and Expansion Pressure of Compacted Soils |
| AASHTO layer coefficient | $M_r = 30000\left(\frac{a_i}{0.14}\right)$ | a _i =AASHTO layer coefficient | AASHTO Guide for the Design of Pavement Structures (1993) |
| PI and Gradation | $CBR = \frac{75}{1 + 0.728(w.PI)}$ | w.PI = P200*PI P200=percent passing No.200 sieve size PI=plasticity index, percent | AASHTO T27-Sieve Analysis of Coarse and Fine Aggregates AASHTO T90-Determining the plastic and Plasticity Index of Soils |
| DCP | $CBR = \frac{292}{DCP^{1.12}}$ | DCP=DCP index, in/blow | ASTM D6951-Standard Test Method for Use of the Dynamic Cone Penetrometer in Shallow Pavement Applications |

Table 2.2 Resilient moduli recommended by the MEPDG based on the soil classification

| AASHTO Symbol | Typical CBR Range | M_R Range (ksi) | M_R Default (ksi) |
|----------------------|--------------------------|----------------------------------|------------------------------------|
| A-7-6 | 1-5 | 2.5-7 | 4 |
| A-7-5 | 2-8 | 4-9.5 | 6 |
| A-6 | 5-15 | 7-14 | 9 |
| A-5 | 8-16 | 9-15 | 11 |
| A-4 | 10-20 | 12-18 | 14 |
| A-3 | 15-35 | 14-25 | 18 |
| A-2-7 | 10-20 | 12-17 | 14 |
| A-2-6 | 10-25 | 12-20 | 15 |
| A-2-5 | 15-30 | 14-22 | 17 |
| A-2-4 | 20-40 | 17-28 | 21 |
| A-1-b | 35-60 | 25-35 | 29 |
| A-1-a | 60-80 | 30-42 | 38 |

The correlations developed by various studies predict the resilient moduli reasonably well for different types of geomaterials in their own inference spaces. However, most models exhibit poor predictive power when they are tested on different soils which are not used to develop the relationships (Von Quintus and Killingsworth, 1998; Yau and Von Quintus, 2002; Wolfe and Butalia, 2004; Malla and Joshi, 2006). Such problems should be expected as correlations are developed from data that may have shown large variations for similar types, similar compaction, and stress conditions. Table 2.3 provides the assessment to

estimate the modulus of geomaterials either through laboratory or field testing or through empirical relationships.

Table 2.3 Assessment of Approaches in Estimating Moduli of Compacted Geomaterials (Puppala, 2008)

| Correlation Type | Reliability | Needs Additional Laboratory Studies for Verification? | Stress Estimation in Bases and Subgrades |
|----------------------------------|----------------------------|--|---|
| Laboratory Determined Parameters | Moderately Reliable | Yes | Not Needed |
| Field Determined Parameters | Moderately Reliable | Yes | Not Needed |
| Indirect Parameters | Low to Moderately Reliable | Yes | Needed |

2.4 Factors Impacting Resilient Modulus of Compacted Geomaterials

There is a consensus on the major factors that could affect the resilient modulus of geomaterials (Puppala, 2008). These generally include the stress state, moisture content (including degree of saturation or suction), stress history, density (including void ratio), gradation (including the percentages of fines) and Atterberg limits (Uzan, 1985; Thom and Brown, 1988; Mohammad et al., 1994a and b; Drumm et al., 1997). The factors that affect resilient modulus are explained in the following section.

2.4.1 State of Stress

The most significant factor that affects the resilient modulus of soils is the state of stress. In coarse grained or granular materials, confining pressure has greater effect on the resilient response than deviatoric stress (Seim, 1989) whereas for fine grained soils the resilient behavior is more dependent on the deviatoric stress than on the confining pressure. The constitutive model used to describe the results of M_R tests is

$$E = k_1 \sigma_c^{k_2} \sigma_d^{k_3} \quad (2-4)$$

The reason for using Equation 2-4 is that, pavement engineers have a better sense for the confining pressure (σ_c) and deviatoric stress (σ_d). The accuracy and reasonableness of this model are extremely important because they are the keys to combine laboratory and field results. Figure 2.3 represents the stress conditions in the field.

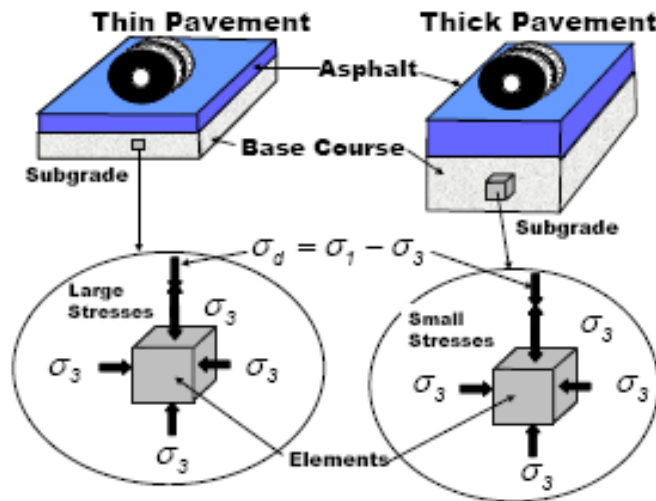


Figure 2.3 Stress level in a pavement (Hopkins et al. 2007)

The so-called two-parameter models advocated by the AASHTO 1993 design guide can be derived from Equation 2-5 by assigning a value of zero to k_2 (for fine-grained materials) or k_3 (for coarse-grained materials). As such, considering one specific model does not impact the generality of the conclusions drawn.

The term $k_1\sigma_c^{k_2}$ in Equation 2-4 corresponds to the initial tangent modulus at a given confining pressure. Since normally parameter k_2 is positive, the initial tangent modulus increases as the confining pressure increases. Parameter k_3 suggests that the modulus changes as the deviatoric stress changes. Because k_3 is usually negative, the modulus decreases with an increase in the deviatoric stress (or strain). The maximum feasible modulus from Equation (2-4) is equal to $k_1\sigma_c^{k_2}$, i.e. the initial tangent modulus.

The state of stress is bound between two extremes, when no external loads are applied and under external loads imparted by a truck. When no external load is applied the initial confining pressure, σ_{c_init} , is:

$$\sigma_{c_init} = \frac{1+2k_0}{3}\sigma_v \quad (2-5)$$

where σ_v is the vertical geostatic stress and k_0 is the coefficient of lateral earth pressure at rest. The initial deviatoric stress, σ_{d_init} can be written as:

$$\sigma_{d_init} = \frac{2-2k_0}{3}\sigma_v \quad (2-6)$$

When the external loads are present, additional stresses, σ_x , σ_y and σ_z , are induced in two horizontal and one vertical directions under the application of

an external load. A multi-layer algorithm can conveniently compute these additional stresses. The ultimate confining pressure, σ_{c_ult} is:

$$\sigma_{c_ult} = \frac{1+2k_0}{3} \sigma_v + \frac{\sigma_x + \sigma_y + \sigma_z}{3} \quad (2-7)$$

and the ultimate deviatoric stress, σ_{d_ult} , is equal to

$$\sigma_{d_ult} = \frac{2-2k_0}{3} \sigma_v + \frac{2\sigma_z - \sigma_x - \sigma_y}{3} \quad (2-8)$$

Under truck loads, the modulus can become nonlinear depending on the amplitude of confining pressure σ_{c_ult} and deviatoric stress of σ_{d_ult} . In that case

$$E = \sigma_{c_ult}^{k_2} \sigma_{d_ult}^{k_3} \quad (2-9)$$

The new mechanistic-empirical design guide (MEPDG) is utilizing the resilient modulus constitutive equation provided in Equation (2-10). The model is generally referred as universal model with its main advantage being the consideration of the stress stage of the material during testing.

$$M_R = k_1 p_a \left(\frac{\theta}{p_a} \right)^{k_2} \left(\left(\frac{\tau_{oct}}{p_a} \right) + 1 \right)^{k_3} \quad (2-10)$$

Where, k_1, k_2, k_3 = material specific regression coefficients, θ = bulk stress,

p_a = atmospheric pressure (i.e., 14.7 psi), and τ_{oct} = octahedral shear stress.

The dependency of the modulus on the state of stress brings about several practical complications in the context of this study. These complications can be summarized into the following items:

- The modulus of a given geomaterial placed in a pavement section is not a unique value and depends on the underlying and/or overlying layers.

- The state of the stress of a given geomaterial placed in a pavement section can only be estimated if the moduli of all layers are known. As such, the estimation of the target modulus based on the design modulus has to be carried out iteratively using an analytical layered structural model (based on linear-elastic layered theory or nonlinear finite element).
- The sophistication of the selected analytical structural model impacts the design and target modulus.

2.4.2 Moisture Content

The impact of the moisture content (or alternatively degree of saturation or suction) is well studied in the literature. Excellent overviews of the impact of moisture content can be found in Richter (2006), Zaman and Khoury (2007) and Cary and Zapata (2010).

Wolfe and Butalia (2004), Hopkins et al. (2004) and Ooi et al. (2006) described the effects of saturation on the resilient moduli of various compacted geomaterials. Figure 2.4 presents a resilient modulus measurement of a subgrade material at different moisture content and related saturation conditions. A decrease of close to 70 MPa was observed in the moduli value when the clayey subgrade was subjected to full saturation from the dry compaction state.

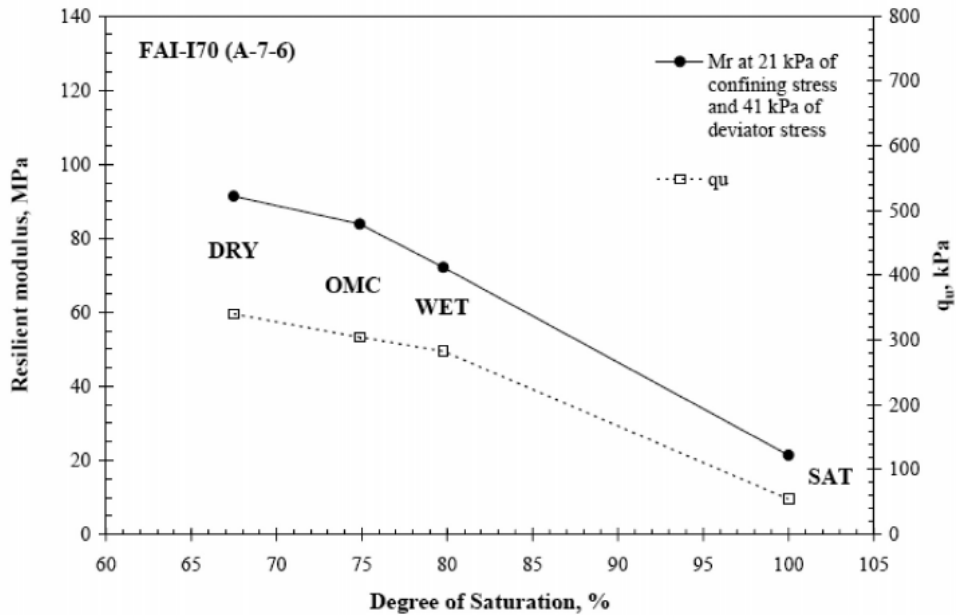


Figure 2.4 Resilient moduli at different saturation conditions (Wolfe and Butalia 2004)

Drumm et al. (1997) investigated the variation of resilient modulus with an increase in post compaction moisture content and proposed a method for correcting the resilient modulus for increased degree of saturation. The resilient modulus at higher saturations is estimated using the gradient of resilient modulus with respect to degree of saturation. Based on that research, the following model was developed for resilient modulus:

$$M_R = k_3 (\sigma_d + X\Psi_m)^{k_4} \quad (2-11)$$

where k_3 and k_4 are regression parameters; M_R = resilient modulus; σ_d = deviatoric stress; Ψ_m = matric suction; and X = function of degree of saturation.

Zaman and Khoury (2007) also focused on evaluating the effect of post-compaction moisture content on the resilient modulus of selected soils in Oklahoma. To test specimens at different suction levels, the authors used wetting

and drying process on samples compacted at predetermined water contents. For example, samples compacted at optimum moisture contents (OMC) were dried to OMC-4% and then wetted to OMC+4%. After the completion of resilient modulus testing, the filter paper tests were performed. Suction tests at various moisture levels were used to establish soil-water characteristic curve (SWCC) profiles. Authors observed that the resilient modulus-moisture content relationships of all the selected soils exhibit a hysteric behavior due to wetting and drying process. The resilient modulus showed an increasing trend with soil suction.

Nazarian and Yuan (2008) determined the layer moduli under different moisture regimes using seismic based nondestructive testing. Laboratory tests were carried out to quantify the moisture susceptibility of the materials. Resilient modulus tests were conducted on soil samples compacted at OMC and then left for drying and wetting process for a span of 15 days. Test results were analyzed to monitor the changes in modulus with moisture content. Nazarian and Yuan observed that:

- Under constant compaction effort, the maximum modulus (M_R) was obtained at a moisture content lower than OMC.
- The difference between the optimum moisture content and the moisture content at which the maximum modulus was determined was dependent on the fine content of the mixture.

According to Cary and Zapata (2010), the effects of the environmental factors on the M_R can be evaluated and expressed as the following function

$$M_R = F_{env} \times M_{Ropt} \quad (2-11)$$

Where F_{env} is the composite environmental adjustment factor and M_{Ropt} is the resilient modulus at optimum conditions and at any state of stress. The model internally used by the MEPDG program to estimate the effect of moisture change is given by:

$$\text{Log} \left(\frac{M_R}{M_{R-opt}} \right) = a + \frac{b-a}{1+EXP(\beta+k_m*(S-S_{opt}))} \quad (2-12)$$

where M_R = modulus at any degree of saturation, S = current degree of saturation (decimal), M_{R-opt} = modulus at OMC and MDD, S_{opt} = degree of saturation at OMC (decimal), a = minimum of $\log(M_R/M_{R-opt})$, b = maximum of $\log(M_R/M_{R-opt})$, β = location parameter as a function of a and $b = \ln(-b/a)$, and K_m = regression parameter.

Hossain (2008) conducted a study for the Virginia DOT to evaluate the use of resilient modulus values in the MEPDG design and analysis. Quick direct shear test was performed at confining pressure of 5 psi at the end of resilient modulus testing to develop correlations between resilient moduli and shear strength properties. To verify the saturation based MEPDG resilient modulus model, a set of samples were compacted and tested at OMC and 20% more moisture than the OMC.

Sawangsurriya et al. (2008) studied matric suction, small strain shear modulus and compaction properties of various soils to present various empirical relations. Various compaction moisture content regimes including dry to wet of optimum with Proctor and reduced Proctor energies were studied. A generalized

relationship among modulus-suction-compaction conditions was developed. Figure 2.5 presents the effects of matric suction on the resilient modulus of subgrade soils tested at various suction conditions. An increase in suction showed an increase in M_R value of the soil because an increase in suction is always associated with dry conditions in the soil specimens.

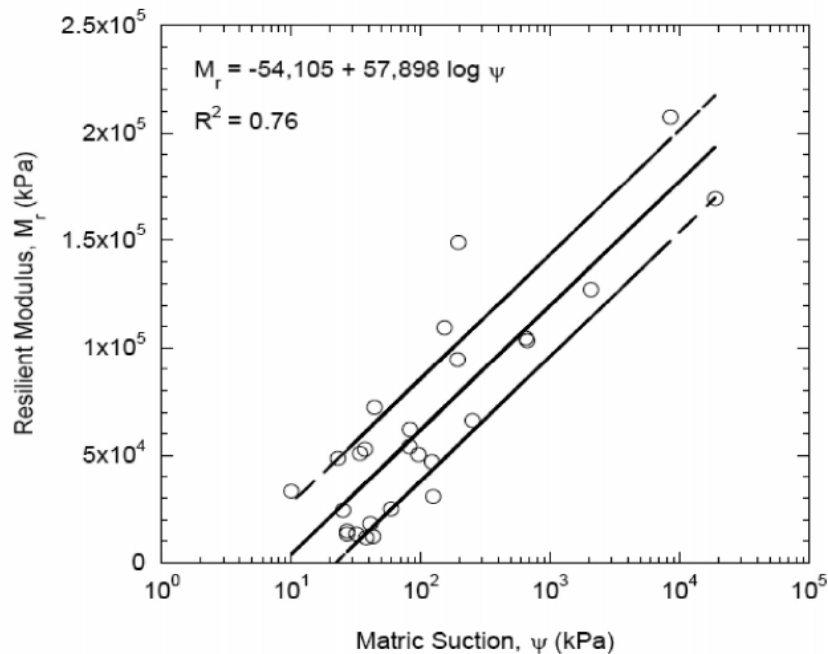


Figure 2.5 Effect of matric suction on resilient modulus (Edil et al. 2006)

Richter (2006) demonstrated a lack of strong relationship between the field modulus and moisture content. Several recent studies including Pacheco and Nazarian, 2011 have focused on explaining this matter. Aside from experimental errors, some of the parameters that are attributed to the lack of the correlations between the modulus and moisture content are variation in densities (Von Quintus et al., 2010 and Pacheco and Nazarian, 2011), significant impact of

the moisture at the time of placement relative to the modulus at the time of field testing (Khoury and Zaman, 2004, Pacheco and Nazarian, 2011).

Siekmeier (2011) based on the compilation of a number of studies proposed the following equation for estimating modulus as a function of moisture content:

$$M_r = k_1 \times p_a \times \left(\frac{\sigma_{eb} + f_s \theta_w \Psi}{p_a} \right)^{k_2} \times \left(\frac{\tau_{oct}}{p_a} + 1 \right)^{k_3} \quad (2-13)$$

where p_a = atmospheric pressure, σ_{eb} = external bulk stress, τ_{oct} = octahedral shear stress, θ_w = volumetric moisture content, θ_{sat} = volumetric moisture content at saturation, and Ψ = matric suction. Siekmeier proposed relationships for estimating parameters k_1 through k_3 and f_s and Ψ for fine-grained soils.

2.4.3 Dry Density

The impact of dry density on modulus has not been studied as extensively as the impact of moisture content since field acceptance of compacted geomaterials in most specifications is based on achieving a certain density. Increase in density should intuitively correlate to increase in modulus. In many field studies a strong correlation between modulus and density could not be found (e.g., Mooney et al., 2009; and Von Quintus et al., 2010). Figure 2.6 presents the measurement of resilient moduli of a base material at various compaction moisture content and dry density conditions.

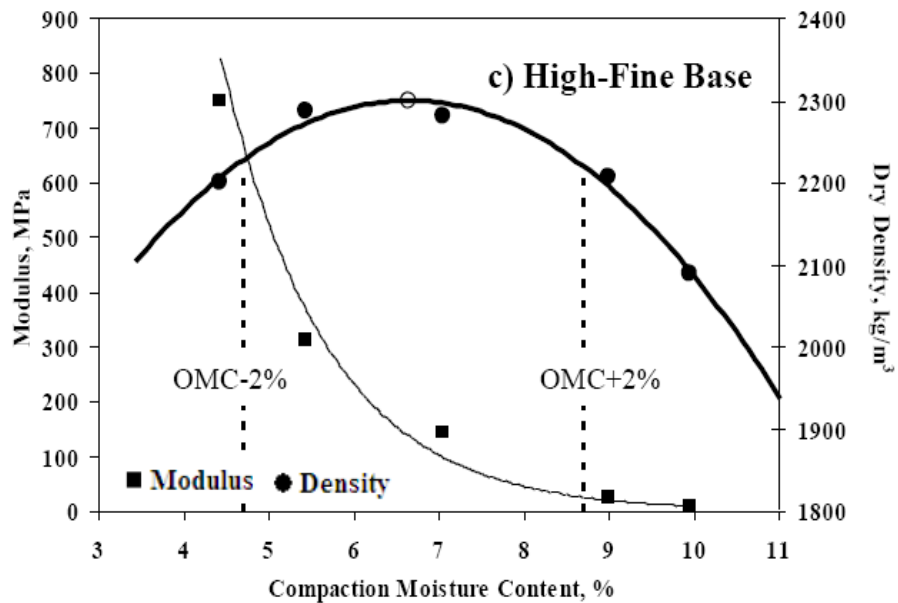


Figure 2.6 Resilient moduli prepared at different densities (Pacheco and Nazarian 2010)

Pacheco and Nazarian (2011) attributed the lack of strong correlation to the differences in the compaction efforts between the field and lab tests and to the complex interaction between the moisture content, dry density and degree of saturation of a given material. In laboratory tests, the maximum dry density is obtained by preparing a series of specimens with different moisture contents and compacting them with a constant energy. Irrespective of the moisture content, the same material is compacted in the field with the minimum number of passes to achieve a desired density. As such, there may be a significant difference in the field and lab compactive energy that may impact the modulus of the materials. To test this concept, Pacheco and Nazarian prepared a number of specimens to the same maximum dry density but with different moisture contents following the Proctor method. The amount of energy to achieve a target density at each

moisture content, which was determined by trial and error, varied from 32 hammer blows (for wet specimens) to more than 90 blows (for dry specimens). The modulus decreased in all cases as the compaction moisture content increased, even though the densities of the specimens were more or less the same. The ratios of the moduli at the dry and wet states varied by as low as 2 for clays to as high as 17 for a high-fines content unbound aggregate base.

2.4.4 Gradation and Plasticity

The impact of gradation and plasticity on modulus have been extensively qualified (see Richter, 2006; Puppala, 2008) and to lesser extent quantified. Table 2.3 contains several relationships developed to quantify the impact of these variables. In general, as the plasticity of the material and the percent fines increases, the modulus decreases.

2.4.5 Long-term and Short-term Behaviors of Geomaterials

In a proper field compaction, the geomaterial is placed near the optimum moisture content and the moisture change is due either evaporation or due to the introduction of moisture. The moduli obtained from this process could be different than the moduli measured in the lab under a constant compaction effort (Khoury and Zaman, 2004; Sabnis et al., 2009 and Pacheco and Nazarian, 2011). This may be the reasons that the past experiences in correlating the laboratory and field moduli have yielded mixed success (Hossain and Apeagyei, 2010).

Table 2.4 Parameters Relating Modulus to Index Properties of Geomaterials

| Model Type | Developed by | Gradation and Plasticity Parameters Included |
|--|----------------------------|---|
| $M_r = k_1 P_a \left(\frac{\theta}{P_a}\right)^{k_2} \left(\frac{\tau_{OCT}}{P_a}\right)^{k_3}$ | Malla and Joshi (2008) | Percent passing 3", 1", $1\frac{1}{2}$ ", #40, #20, #200 sieves Percent fine sand C_U =Uniformity coefficient C_C = Coefficient of curvature |
| $M_r = k_1 P_a \left(\frac{\theta}{P_a}\right)^{k_2} \left(\frac{\sigma_d}{P_a}\right)^{k_3}$ | Santha (1994) | Percent passing sieve #40 Percent of silt and clay Percent of swell and shrinkage Liquid limit and plastic limit |
| $M_r = k_1 P_a \left(\frac{\theta}{P_a}\right)^{k_2} \left(\frac{\sigma_d}{P_a}\right)^{k_3}$ | Glover and Fernando (1995) | Liquid limit and plastic limit Specific gravity of soil binder Percent passing sieve #40 Dialectic constant |
| $\frac{M_r}{\sigma_{atm}} = K_1 \left(\frac{\sigma_{oct}}{\sigma_{atm}}\right)^{k_2} \left(\frac{\tau_{oct}}{\sigma_{atm}}\right)^{k_3}$ | Mohammad (1999) | Liquid limit and plastic limit |
| $M_r = k_1 P_a \left(\frac{\theta}{P_a}\right)^{k_2} \left(\frac{\tau_{OCT}}{P_a} + 1\right)^{k_3}$ | Amber (2002) | Percentage passing sieve # $\frac{3}{8}$, #4, #40 Liquid limit and plastic limit |

Significant work has been done to predict the long-term changes in the moisture content/suction and modulus of the compacted geomaterials under the in service pavement. However, the amount of work related to short term behavior of exposed geomaterials (as related to the quality management has been limited).

The Enhanced Integrated Climatic Model (EICM) is an integral part of the Mechanistic Empirical Pavement Design Guide (MEPDG), and perhaps the most common algorithm used for predicting the long term change in modulus of compacted soils. EICM involves analysis of moisture and heat flow through different pavement layers under different boundary conditions. One of the main functions of the EICM in the MEPDG design guide is to evaluate the relationships between the change in water content and mechanical properties of unbound pavement layers.

The EICM estimates the change in water content in the pavement layers, the drainage and conductivity characteristics of the layers, and the water storage capacity of each layer, based on the boundary conditions on the ground surface, the depth of moisture change zone, and equilibrium moisture content (or suction), and initial conditions. The current EICM uses empirical relationships between the modulus of compacted soils and the degree of saturation.

The EICM consists of four major parts: The Precipitation (PRECIP) model, the Infiltration and Drainage (ID) model, the Climatic-Material-Structural Model (CMS) model, and the U.S. Army Cold Regions Research and Engineering Laboratory (CRREL) model for Frost Heave-Thaw Settlement. These models are integrated to some extent through the use of some common boundary conditions with typical inputs and outputs (Zapata 2009). Since each of these models was originally developed as a separate program for a specific use, there is significant

amount of overlap between the functions, capabilities, and limitations of these models (McCartney et al. 2010).

Zapata and Houston (2008) conducted a comprehensive study to incorporate new empirical relationships into the EICM for the saturated hydraulic conductivity and the SWCC for further improvement of the EICM model. The study involved collection of soils from 30 sites throughout the US, collection of weather data from online databases for these sites, and prediction of the water content from the sites using the EICM. The study also involved comparing the predicted water content from the EICM with field measurements. Although this extended database improved the capabilities of the EICM model, the current MEPDG empirical equation that correlates the resilient modulus and degree of saturation with the regression fitting parameters, do not consider the effects of mechanical stress on the resilient modulus in detail.

More recent studies have focused more on the combined effects of the two stress state variables as adopted in unsaturated soil mechanics (i.e., suction and mechanical stress). Gupta et al. (2007) observed a more consistent trend between resilient modulus and suction at constant confining stresses. Suction and degree of saturation relationship for each soil is unique and is established through the SWCC. As such, the degree of saturation (or water content) may not be the primary variable affecting the resilient modulus. In other words, the degree of saturation for different soils at the same suction may be different.

Nevertheless, it may be more practical to consider moisture content or degree of saturation in the day-to-day protocols to be implemented by highway agencies.

2.5 Summary

This chapter reviewed the research conducted on the resilient modulus parameter of unsaturated soils. Previous literature cited on resilient modulus theory is presented in this chapter. The literature review covered the concept of resilient modulus followed by estimation of modulus using the three levels (laboratory tests, field tests and correlations). The last section explains the factors which impact the modulus were presented. In the next chapter detailed test procedures followed in the current research are presented.

CHAPTER 3

EXPERIMENTAL PROGRAM

3.1 Introduction

This experimental program was designed and conducted to determine the resilient properties of the base material specimens compacted at five different moisture content-dry density conditions. The following sections describe the physical properties and testing materials used in this research, types of laboratory tests performed, test equipment, and the test procedures adopted.

3.2 Basic Soil Tests

The base materials used in this research are unbound material obtained from El Paso and Austin. The basic tests included grain size distribution tests, specific gravity, and proctor compaction tests. The basic testing was done in accordance with the current TxDOT and AASHTO standard testing procedures.

3.2.1 Basic Soil Properties

The basic soil tests conducted for this research project included sieve analysis, specific gravity tests, and Atterberg limit tests. As per Tex-110-E method, sieve analysis test was conducted to obtain the grain-size distribution of soils. Sieve analysis provides the percent amount of various size fraction of the soil including percent fines. The distribution of particle size of the soil retained on No.200 sieve is determined by sieve analysis.

3.2.2 *Atterberg Limits*

Upon addition of water, the states of soil changes from dry, semi-solid, plastic and finally to liquid limit states. The water content at the boundaries of these states are known as shrinkage (SL), plastic (PL) and liquid (LL) limits, respectively (Lambe and Whitman, 2000). Also known as Atterberg limits, the above mentioned soil properties are essential to correlate the shrink-swell potential of the soils to their respective plasticity indices. LL is known as the water content at which the soil flows and PL is determined as the water content at which the soil starts crumbling when rolled into a 1/8-inch diameter thread. The numerical difference between LL and PL is known as plasticity index (PI) and characterizes the plasticity nature of the soil. Representative soil specimens from different locations as mentioned before were subjected to Atterberg limit tests to determine LL and PL following Tex-104-E and Tex-105-E, respectively.

Table 3.1 shows the results of the sieve analysis of the El Paso and Austin soils. Table 3.2 summarizes the physical properties that were evaluated as a part of this research. Depending on the gradation, both the El Paso and Austin soils were classified as GP as per the USCS classification method. The specimens for UCS and Resilient Modulus tests were prepared from the percentages of gravel, sand and fines given in the Table 3.2. Figure 3.1 presents the grain size distribution of El Paso and Austin base material.

Table 3.1 Sieve Analysis

| Sieve | Opening (mm) | Percent Passing | |
|------------|--------------|-----------------|--------|
| | | El Paso | Austin |
| 1" | 25.4 | 100 | 100 |
| 7/8" | 22.4 | 93 | 98 |
| 3/8" | 9.52 | 55.8 | 83.3 |
| #4 | 4.75 | 40.3 | 69.7 |
| #40 | 0.425 | 17.8 | 26.3 |
| #100 | 0.15 | 9.2 | 8.5 |
| #200 | 0.075 | 4.6 | 2.8 |
| Pan (-200) | 0 | 0 | 0 |

Table 3.2 Basic Soil Properties

| Soil Properties | El Paso | Austin |
|---------------------|---------|--------|
| Gravel % | 50 | 30 |
| Sand % | 45 | 67 |
| Fine % | 5 | 3 |
| Liquid Limit | 22 | 27 |
| Plasticity Index | 9 | 14 |
| Specific Gravity | 2.8 | 2.73 |
| USCS Classification | GP | GP |

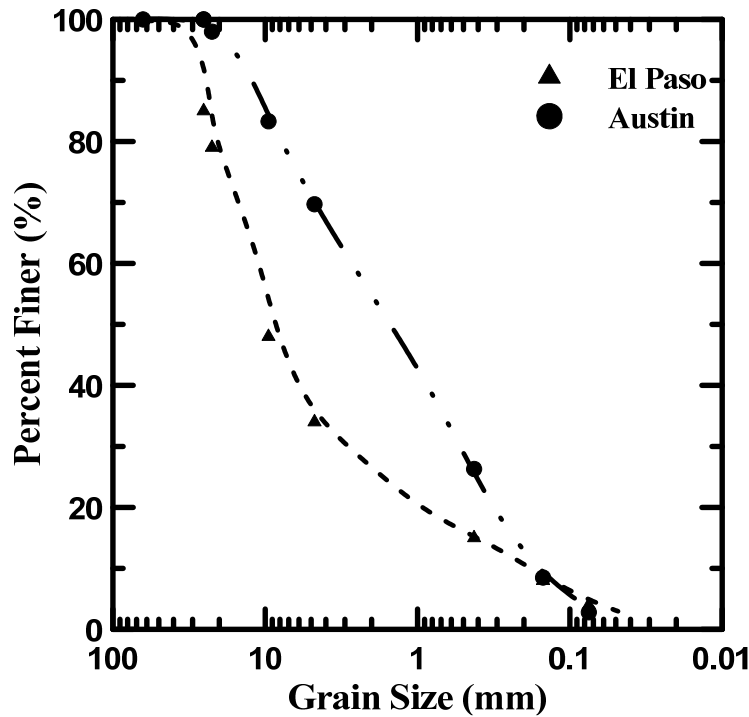


Figure 3.1 Grain Size Distribution

3.2.3 Modified Proctor compaction tests

Modified proctor compaction tests were conducted on El Paso and Austin soil samples to establish the optimum moisture content and dry unit weight relationships. The optimum moisture content of the soil is the water content at which the soils were compacted to a maximum dry unit weight condition. Specimens exhibiting a high compaction unit weight are best in supporting civil infrastructure due to low volume of voids (Pedarla, 2009). Tests were conducted as per the TxDOT procedure (Tex-113-E) for determining the laboratory compaction characteristics and moisture-density relationships. This procedure requires a compactive effort of 13.26 ft-lb/in³. Based on this requirement, for a

4.54 kg (10 lb) weight of hammer and a height of drop of 0.46 m (1.5 ft), it was determined that three layers with 17 blows per layer are required to compact a specimen size of 101.6 mm in diameter and 116.3 mm in height. Table 3.3 presents the compaction parameters adopted for aggregate specimen preparation. Figure 3.2 below presents the compaction dry unit weight and moisture content relationships of El Paso and Austin base materials. The results of this compaction test were adopted in preparing the samples at the five different moisture contents with their respective dry unit weights.

Table 3.3 Compaction Parameters

| | |
|---|--------|
| Required Compactive Effort (ft-lb/in ³) | 13.26 |
| Weight of Hammer (kg) | 4.54 |
| Height of Drop (m) | 0.46 |
| Diameter of Sample (cm) | 10.16 |
| Height of sample (cm) | 11.63 |
| Volume of Molded Specimen (cm ³) | 943.06 |
| No. of Layers | 3 |
| Drops per Layer | 17 |
| Applied Compactive Effort (ft-lb/in ³) | 13.29 |

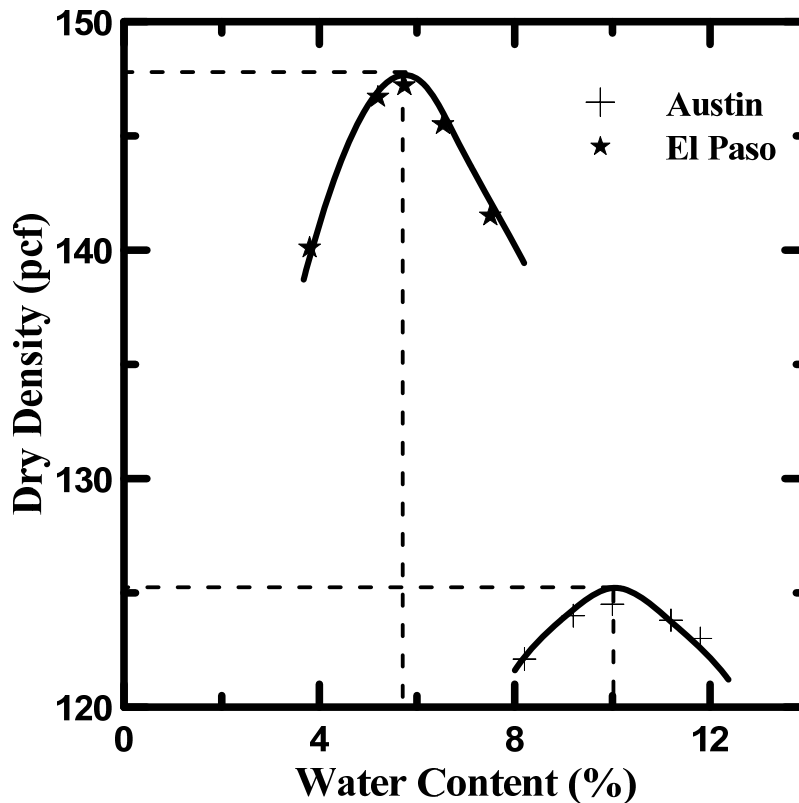


Figure 3.2 Compaction Curve

The maximum dry density and optimum moisture content for the El Paso base is 147 pcf and 6% respectively. Whereas for the Austin base material, the maximum dry density is 125 pcf and optimum moisture content is 10%.

3.3 Advanced Soil Tests

The advanced soil tests conducted in this research are unconfined compressive strength, conventional resilient modulus and suction controlled resilient modulus. Soil water characteristic curve (SWCC) was determined using Tempe cell (Fredlund device). All these advanced testing were conducted on the compacted base specimens.

3.3.1 Specimen Preparation Procedure

The specimens to determine SWCC were prepared at three moisture content-dry density conditions, one at OMC, one on the dry side of OMC (OMC-2%) and one on the wet side of OMC (OMC+2%). Figure 3.3 presents the points at which the specimens were prepared. The dry soil weight for each specimen was calculated from the respective dry unit weight based on the gradation. Specimens of 2.5 inch in diameter and 1 inch thick were compacted with a constant strain rate using static compaction equipment.

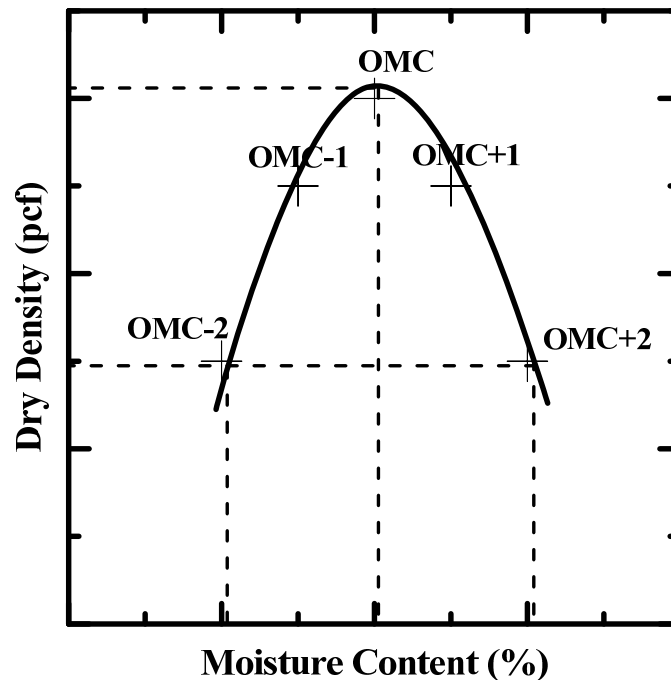


Figure 3.3 Sample Preparation Points for SWCC

Base specimens for Unconfined Compressive Strength (UCS) and Resilient Modulus testing have been compacted at five different moisture contents (OMC-2%, OMC-1%, OMC, OMC+1% and OMC+2%) at their respective dry density as presented in Table 3.4.

Table 3.4 Sample Preparation Points for UCS and M_R Testing

| Specimen No. | El Paso | | Austin | |
|--------------|---------------|----------------------|---------------|----------------------|
| | Density (pcf) | Moisture Content (%) | Density (pcf) | Moisture Content (%) |
| 1 | 147 | 6 | 125 | 10 |
| 2 | 145 | 5 | 124 | 9 |
| 3 | | 7 | | 11 |
| 4 | 142 | 4 | 122 | 8 |
| 5 | | 8 | | 12 |

The samples for unconfined compressive strength and resilient modulus tests were compacted in three layers, with 17 drops per layer in a 71 mm in diameter by 142 mm in height mold, conforming to the required compactive effort (13.26 ft-lb/in³) as specified by TxDOT. After compaction, the specimens have been extruded and were kept in the humidity room for one day for uniformity distribution of moisture in the specimen and then tested.

3.3.1.1 Saturation Process

The prepared specimens were placed in the stainless mold and were saturated in de-ionized water for one day. Before saturation the specimen were clamped with two iron plates one on the top and one on the bottom to restrict the volume change. Figure 3.4 shows the specimen saturation process. The saturation process is carried out in the following steps.

- i. De-ionized water was filled till the half the height of the sample and left for 10 to 12 hours.

- ii. After initial saturation, the sample is completely submerged in the water for a period of 12 hours.

The importance of this process is to remove any entrapped air in the sample, which ensures chances of fully saturation in the sample. After saturation, the specimen with the mold is immediately placed on the ceramic disk. The cap was placed and tightened and air pressure was applied to the samples.



Figure 3.4 Saturation of a Sample

3.3.2 Soil Water Characteristic Curve

The soil water characteristic curve represents the relationship between volumetric or gravimetric water content and matric suction for a soil. The water content can be defined as the amount of water contained within the pores of the soil. In soil science volumetric water content (Θ), which is defined as the ratio of volume of water to the total volume of soil is most commonly used (Leong and Rahardjo, 1996). In geotechnical engineering practice, gravimetric water content (ω), which is the ratio of the mass of water to the mass of solids, is most commonly used. (Thudi, 2006)

Matric suction is the capillary component of free energy and is the major contributor to the total suction as osmotic suction arising from salt solutions in a soil is typically small. In general, matric suction is the difference between pore air pressure and pore water pressure. Matric suction is generally related to the surrounding environment and it may vary from time to time. The recent advances in the design of pavements including mechanistic pavement design guide (MEPDG) has emphasized the importance of unsaturated soil properties and the role of matric suction on the subgrade stiffness property, resilient modulus, and its use in the pavement design (Puppala et al. 2012).

Tempe cell was used in this research to study the Soil Water Characteristic Curve (SWCC), for the soils. Tempe cell which is also known as the Fredlund SWCC setup is a simple unsaturated soil testing apparatus with great flexibility for applying matric suctions. Tempe cell works on the principle of axis translation technique, which involves the soil matric suction in different steps and measuring the resulting water content after equilibrium is reached at each air pressure applied.

A soil specimen was placed on top of a saturated ceramic disk. The Ceramic Disk was used to allow the flow of water under applied pressure but impeding the air flow through it. Separation of the air and water pressure is maintained as long as the applied air pressure is less than the air entry pressure of HAE ceramic disk. Figure 3.5 (a) presents the GCTS setup used in this

research. The mounted ceramic stone used in this study has a capacity of 5 bar (500 kPa). Figure 3.5 (b) shows the saturation of a mounted ceramic disk.



(a)



(b)

Figure 3.5 (a) Tempecell setup used in this research (b) Saturation process of HAE Disk

This device includes a pressure panel with dial gauges and regulators. The main functions of these pressure regulators are to apply pore-air pressure (u_a) to the soil specimen. The base has two external ports which connect the volumetric column to measure the water extracted from the soil specimen. This apparatus allows the use of single soil specimen to obtain the entire SWCC with any number of data points. The air pressures used in this study were 10 kPa, 50 kPa, 100 kPa, 200 kPa, 300 kPa and 450 kPa were applied to get the drying path of SWCC.

After the specimen was placed in the Tempecell setup, the system was flushed before applying the air pressure on the saturated specimen. The flushing process consists of pushing de-ionized water through the spiral compartment below the ceramic disk. The water was flushed back and forth until no air bubbles were observed.

3.3.3 Unconfined Compressive Strength (UCS) Procedure

The unconfined compressive strength (UCS) tests were conducted at the five moisture content - dry density points as described in the above Table 3.4. In this test, cylindrical specimens of 2.8 in. (71 mm) in diameter and 5.6 in. (142 mm) in height were prepared. The testing setup consists of a circular base with a central pedestal. A triaxial cell is fitted to the top of the base plate with the help of 3 wing nuts.

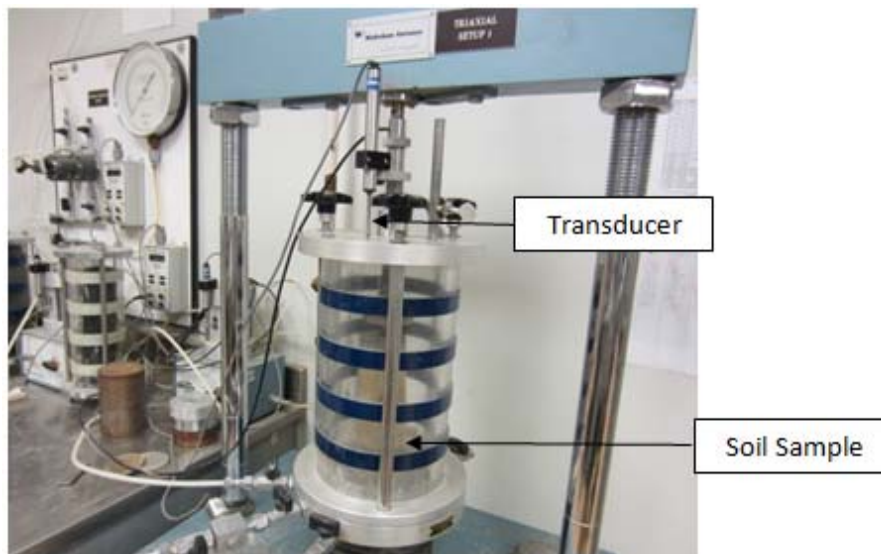


Figure 3.6 Triaxial Equipment

Figure 3.6 presents the triaxial setup used in this study. The triaxial cell is a perplex cylinder which is permanently fixed to the top cap and the bottom brass collar. After the specimen is placed inside the cell soil sample is sheared at a constant strain rate with the help of a loading ram. A graph is plotted between stress vs strain corresponding to the values of load and deformation readings. The maximum axial compressive load, at which the sample failed, was recorded as the unconfined compressive strength of the samples.

3.3.4 Conventional Resilient Modulus Test Procedure

The Resilient Modulus Test using the Cyclic Triaxial test equipment is designed to simulate the traffic wheel loading on the in situ soils by applying a sequence of repeated or cyclic loading on the soil specimens. In this research, the 'standard method of testing for determining the resilient modulus of soils and aggregate materials – AASHTO Designation T 307-99' has been employed. The stress levels used for testing the soil specimens are based upon the location of the specimen within the pavement structure as standardized by AASHTO for Base/Subbase materials. Water was used as the confining medium. Loading and cell pressures were controlled automatically through the data acquisition system.

Table 3.5 below presents the testing sequence employed in the procedure. The confining pressure typically represents overburden pressure of the specimen location in the subgrade. The axial deviatoric stress is composed of two components, cyclic stress, which is the applied deviatoric stress and a contact stress, typically represents a seating load on the soil specimen. It should

be noted that the contact stress is typically equivalent to 10% of overall maximum axial stress.

Table 3.5 Resilient Modulus Testing Sequence

| No. | Confining Pressure | | Max. Axial Stress | | Cyclic Stress | | Contact Stress | | No. of Load Cycles |
|-----|--------------------|------------|-------------------|------------|---------------|------------|----------------|------------|--------------------|
| | <i>kPa</i> | <i>psi</i> | <i>kPa</i> | <i>psi</i> | <i>kPa</i> | <i>psi</i> | <i>kPa</i> | <i>psi</i> | |
| 0 | 103.4 | 15 | 103.4 | 15 | 93.1 | 13.5 | 10.3 | 1.5 | 500-1000 |
| 1 | 20.7 | 3 | 20.7 | 3 | 18.6 | 2.7 | 2.1 | 0.3 | 100 |
| 2 | 20.7 | 3 | 41.4 | 6 | 37.3 | 5.4 | 4.1 | 0.6 | 100 |
| 3 | 20.7 | 3 | 62.1 | 9 | 55.9 | 8.1 | 6.2 | 0.9 | 100 |
| 4 | 34.5 | 5 | 34.5 | 5 | 31 | 4.5 | 3.5 | 0.5 | 100 |
| 5 | 34.5 | 5 | 68.9 | 10 | 62 | 9 | 6.9 | 1 | 100 |
| 6 | 34.5 | 5 | 103.4 | 15 | 93.1 | 13.5 | 10.3 | 1.5 | 100 |
| 7 | 68.9 | 10 | 68.9 | 10 | 62 | 9 | 6.9 | 1 | 100 |
| 8 | 68.9 | 10 | 137.9 | 20 | 124.1 | 18 | 13.8 | 2 | 100 |
| 9 | 68.9 | 10 | 206.8 | 30 | 186.1 | 27 | 20.7 | 3 | 100 |
| 10 | 103.4 | 15 | 68.9 | 10 | 62 | 9 | 6.9 | 1 | 100 |
| 11 | 103.4 | 15 | 103.4 | 15 | 93.1 | 13.5 | 10.3 | 1.5 | 100 |
| 12 | 103.4 | 15 | 206.8 | 30 | 186.1 | 27 | 20.7 | 3 | 100 |
| 13 | 137.9 | 20 | 103.4 | 15 | 93.1 | 13.5 | 10.3 | 1.5 | 100 |
| 14 | 137.9 | 20 | 137.9 | 20 | 124.1 | 18 | 13.8 | 2 | 100 |
| 15 | 137.9 | 20 | 275.8 | 40 | 248.2 | 36 | 27.6 | 4 | 100 |

A haversine-shaped wave load pulse with a frequency of 10 Hz was applied as the traffic wheel loading on the soil. A loading period of 0.1 sec and a

relaxation period of 0.9 sec were used in the testing. These loading features are in accordance with the resilient modulus test procedure outlined in AASHTO T 307-99 procedure. The selection of haversine load is recommended in AASHTO procedures based on the road test research performed in the USA.

As presented in Table 3.5, the test process requires both conditioning followed by actual testing under a magnitude of confining pressure and deviatoric stresses. At each confining pressure and deviatoric stress, the resilient modulus value was determined by averaging the resilient deformation of the last five deviatoric cycles. Hence, from a single test on a compacted soil specimen, several resilient moduli values at different combinations of confining and deviatoric stresses were determined.

3.3.5 Suction Controlled Resilient Modulus Testing

The conventional resilient modulus testing was modified to suction controlled resilient modulus testing to account the unsaturated soil phenomena. The conventional bottom platen was replaced by pedestal fitted with a ceramic disk. One more modification was the addition of external line for air pressure supply.

There are two approaches to perform resilient modulus tests under controlled suction conditions. The first approach was to induce controlled soil suction conditions by axis translation technique. For unsaturated resilient modulus testing, air pressure (u_a) was applied from the top of the specimen and the water pressure (u_w) was left to atmosphere (here $u_w=0$). Figure 3.7 shows the

schematic of the equipment used in this study. The cell has the following features:

1. In this testing system the pore air pressure was controlled manually and applied directly on the lateral surface of the specimen.
2. The pore water was freely drained from the bottom of the specimen through the pedestal fitted with a ceramic disk.

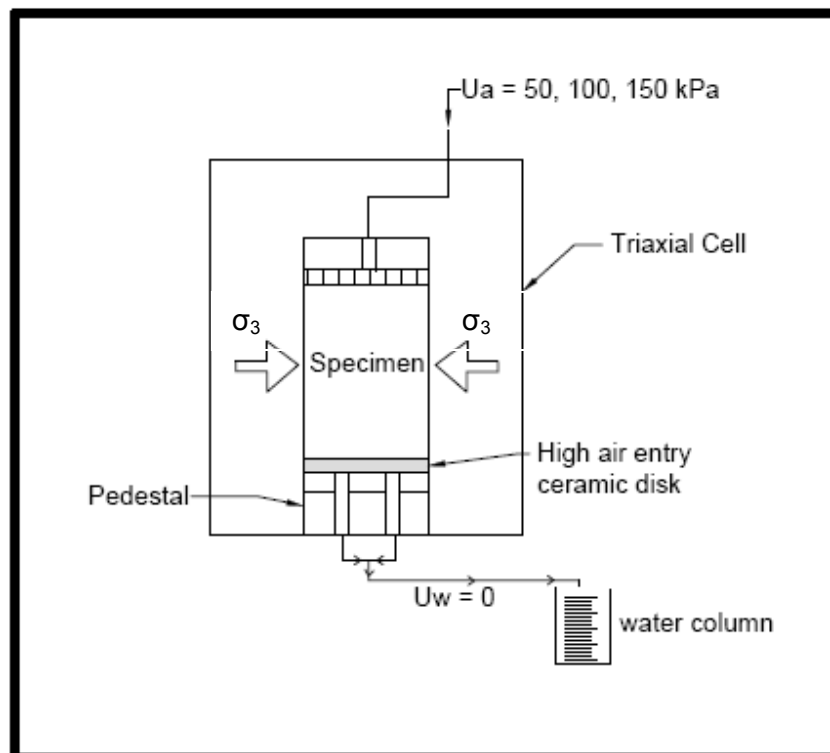


Figure 3.7 Unsaturated Resilient Modulus Testing Equipment

To achieve equilibration in the specimen confining pressure was applied higher than the air pressure. The saturated specimen was placed in contact with the saturated ceramic disk. Water was drained from the specimen until it reaches the equilibrium stage at that applied air pressure. Two water lines from the

loading frame were connected to the two water columns of the Tempe cell to read the water volume change in the specimen. Once the equilibrium stage has reached the specimen was tested for two confining pressures and five deviatoric loads.

The conventional resilient modulus test is based on total stress approach in which the specimens were subjected to different combinations of deviatoric cyclic stress and total confining pressures. But for suction controlled resilient modulus tests, taking into account of unsaturated soil mechanics approach, the air phase becomes important in the measurement and control of matric suction. Therefore the total stress is replaced by the net normal stress which is the difference of total normal stress and pore air pressure. Table 3.6 provides the net pressures used for suction controlled resilient modulus testing. The five deviatoric stress applied were 35, 68.9, 103.4, 137.9 and 206.8 kPa.

Table 3.6 Cell Pressure, Pore-Air Pressure for Suction Controlled M_R Testing

| σ_3 (kPa) | | u_a (kPa) | u_w (kPa) | $\sigma_3 - u_a$ (kPa) | | $\psi = u_a - u_w$ (kPa) |
|------------------|-----|-------------|-------------|------------------------|----|--------------------------|
| 85 | 120 | 50 | 0 | 35 | 70 | 50 |
| 135 | 170 | 100 | 0 | 35 | 70 | 100 |
| 185 | 220 | 150 | 0 | 35 | 70 | 150 |

The only limitation of this approach was that it will take a longer time to reach equilibrium conditions once a soil suction state is induced. An attempt was made to perform this approach and compare the results with the second approach.

The second approach was to monitor the soil suction during the resilient modulus testing which in turn explains the changes in soil suction during repeated loading. Initial soil suction condition was established based on the soil water characteristic curve information and the initial compaction moisture conditions. Since the tests are non-destructive in nature, the initial suction conditions were expected to prevail during testing. Hence the proposed resilient modulus testing was achieved by varying initial moisture conditions in the compacted soil samples which represents various suction conditions

3.4 Equipment Employed for the Resilient Modulus Testing

The RMT was conducted using the UTM-5P dynamic triaxial system. The UTM-5P is a closed loop, servo control, materials testing machine and is designed to facilitate a wide range of triaxial testing. The major components of UTM-5P system are loading frame, controller and data acquisition system.

3.4.1 *Loading Frame*

The loading frame consists of a heavy flat base plate, supported on four leveling screws. Two threaded rods support the crosshead beam and provide height adjustment. The frame is of heavy construction to limit deflection and vibrations that could influence the accuracy of measurements during dynamic repeated loading tests. The loading forces are applied through the shaft of a pneumatic actuator mounted in the centre of the crosshead. Sensitive, low friction displacement transducers attached to the crosshead enable

measurement of the permanent and small resilient deflections of the specimen during loading. The loading frame is as shown in the Figure 3.8 below.



Figure 3.8 The Loading Frame and Triaxial Cell

3.4.2 *The pneumatic loading system*

The UTM pneumatic system is an air compressor controller unit used to control both load and pressures applied on soil specimens. For asphalt tests, only the vertical force pneumatics is required, while the unbound tests on soils require both confining and axial deviatoric pressure pneumatics. The system requires a filtered clear air supply at a minimum supply pressure of 800 kPa. Lower supply pressures will prevent the system from achieving the maximum specified stresses or forces, as selected by the operator. Figure 3.9 shows the Pneumatic system at the UTA geotechnical lab facility.



Figure 3.9 The Pneumatic System

3.4.3 *Triaxial Cell*

The triaxial pressure cell used is suitable for testing specimens having dimensions of upto 200 mm height by 100 mm diameter. This unit is rated to a maximum confining pressure of 1700 kPa. To provide maximum visibility, the cell chambers are made of Lucite-type material. The cell is designed to contain pressurized liquid only and so the use of any compressible gas as a confining medium is dangerous.

3.4.4 *Control and Data Acquisition System*

The UTM Control and Data Acquisition System (CDAS) is a compact, self-contained unit that provides all critical control, timing and data acquisition functions for the testing frame and transducers. The CDAS consists of an Acquisition module (analog input/output) and a Feedback Control module (analog

input/output). The Acquisition module has eight normalized transducer input channels that are digitized by high speed 12 bit Analog to Digital (A/D) converters for data analysis and presentation. In addition two 14 bit Digital to Analog (D/A) converters are available to provide computer control of the voltage to pressure converters. The air pressure is controllable over the range 0 – 700 kPa. There are two output channels provided for applying confining pressures. The SOL1 is used as the trigger input to the feedback control module that creates and controls the waveform. The SOL2 output is used for the digital control signal from computer to control the confining pressure solenoid for triaxial tests.

The Feedback Control module has three normalized input channel controls. These channels are dedicated to the actuator position, actuator force and general purpose input (Aux) for on-specimen transducers. This module has a dedicated communication interface of its own that provides for an uninterrupted, simultaneous communication with the PC enabling increased speed of operation and flexibility. The figure 3.10 below shows the control and data acquisition system.



Figure 3.10 The Control and Data Acquisition System

3.4.5 Linear Variable Displacement Transducers (LVDTs)

Based on the AASHTO testing procedure T 307-99, high resolution LVDTs are needed to measure the soil displacements. Two LVDTs are used to record the vertical displacements. This external displacement transducer is easy to install and provides a simplified procedure to reset the initial zero reading. The LVDTs are placed on the top cover of the cell and fitted to the load shaft. The maximum scale stroke for these two LVDTs is +5 mm, with a resolution of 0.001 mm accuracy. The output from each LVDT is monitored independently and compared to the output of the other LVDTs. Figure 3.11 shows the external transducer assembly employed in this project.

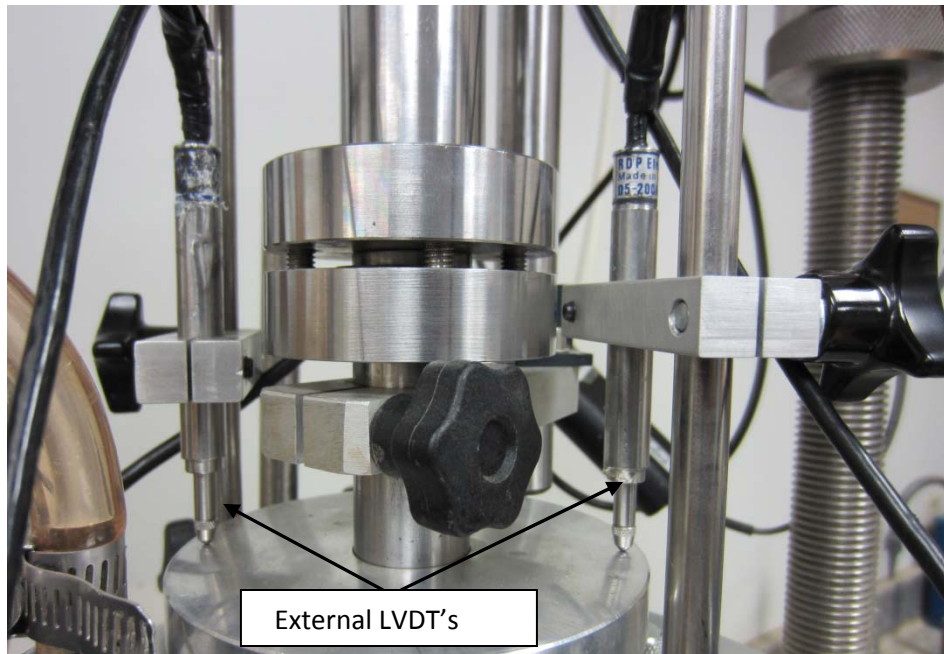


Figure 3.11 External LVDTs Assembly

3.4.6 Software

The UTM software is used for equipment control and data acquisition operations. In this software, there are programs available for several test procedures, which include unconfined compressive strength test, resilient modulus test, unconsolidated undrained test, consolidated undrained test, consolidated drained test and a provision for user defined programs. The user program is a program that is provided for operators to create their own testing methods and protocols. In this Research, the AASHTO T 307-99 program for the determination of resilient modulus of aggregate base materials has been used. The figure 3.12 below shows a sample test data window during the test.

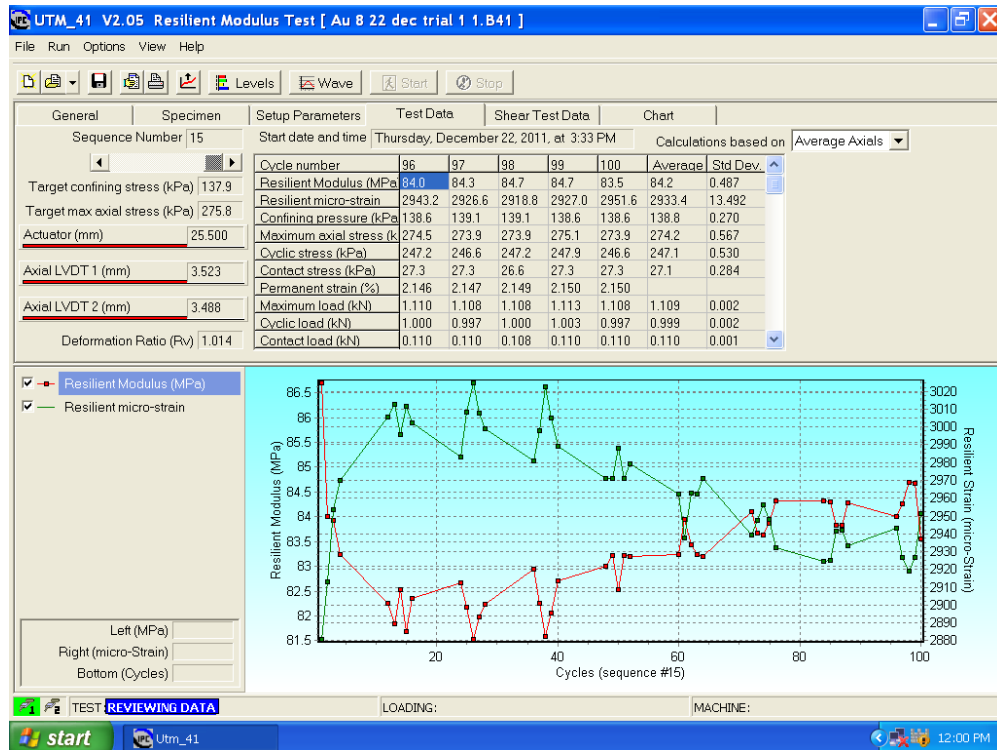


Figure 3.12 Software window showing the test data

3.5 Summary

This chapter provides a summary of basic properties of selected base material, and procedures of advanced soil testing used in this research. Details of the resilient-Strain modulus test procedure employed in this research have also been presented. Also, the notations used to present these test results in a simple format have been explained. The next chapter present the results obtained from the above mentioned tests that were conducted on the two base materials selected for this study.

CHAPTER 4

ANALYSIS OF STRENGTH AND RESILIENT MODULUS TEST RESULTS

4.1 Introduction

This chapter mainly discusses the behavior of the two base materials tested under different tests including unconfined compressive strength, and resilient modulus tests. In the case of resilient modulus testing, the influence of matric suction on test results are addressed by performing both suction controlled resilient modulus testing and conventional resilient modulus testing. For UCS and M_R testing, specimens were tested at five different moisture content and dry density conditions. Also, soil water characteristic studies were determined by testing same soils at three different moisture content and dry density conditions including one at dry, one at optimum and one at wet of optimum conditions.

This chapter also provides the regression analysis attempted on the resilient modulus test results. Modified Universal model and Cary and Zapata models are used to model the measured resilient modulus results. Additionally, a step wise procedure used in MEPDG program is used, to obtain the SWCC of the present materials. Fredlund and Xing equation was used in this procedure. A comparison of predicted SWCC with the measured results is made to evaluate the capabilities of SWCC predictions by the MEPDG model.

4.2 Unconfined Compressive Strength

Unconfined Compression Strength (UCS) tests were performed on the base materials at five moisture content – dry density points. The five moisture density points are clearly explained in Table 3.4. Samples were compacted in a 2.8 x 5.6 in. (diameter × height) mold and were kept at a controlled environment for one day to facilitate the uniform distribution of moisture content in the sample. Later, the specimens were tested under unconfined conditions. Tables 4.1 and 4.2 present the unconfined compressive strength test results of both El Paso and Austin base material specimens, compacted at five different moisture content and dry density conditions.

Table 4.1 UCS test results of El Paso base material

| S.No | El Paso | | | |
|--------|-----------------------------|------------------------------|-------------------|-----------|
| | Target Moisture Content (%) | Nominal Moisture Content (%) | Dry Density (pcf) | UCS (psi) |
| OMC-2% | 4 | 3.8 | 140 | 76 |
| OMC-1% | 5 | 5.2 | 146.7 | 55 |
| OMC | 6 | 5.74 | 147.2 | 38 |
| OMC+1% | 7 | 6.53 | 145.5 | 12 |
| OMC+2% | 8 | 7.5 | 141.5 | 10 |

Table 4.2 UCS test results of Austin base material

| S.No | Austin | | | |
|--------|-----------------------------|------------------------------|-------------------|-----------|
| | Target Moisture Content (%) | Nominal Moisture Content (%) | Dry Density (pcf) | UCS (psi) |
| OMC-2% | 8 | 8.2 | 122.1 | 49 |
| OMC-1% | 9 | 9.2 | 124 | 64.5 |
| OMC | 10 | 10 | 124.5 | 51 |
| OMC+1% | 11 | 11.2 | 123.8 | 44.5 |
| OMC+2% | 12 | 11.8 | 123 | 49.5 |

Figures 4.1 and 4.2 present the unconfined compressive strength test results of both El Paso and Austin materials.

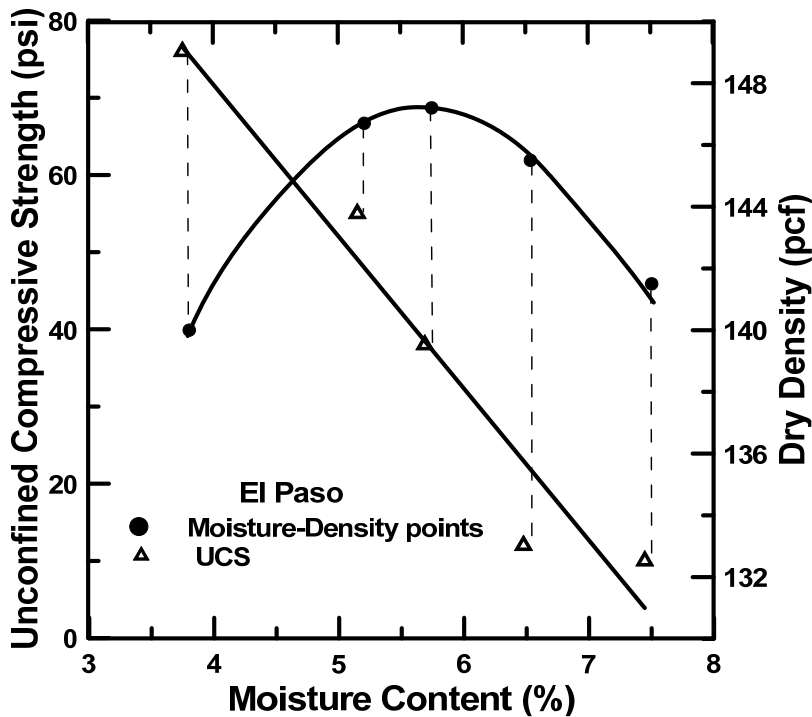


Figure 4.1 Unconfined Compressive Strength Results of El Paso specimens

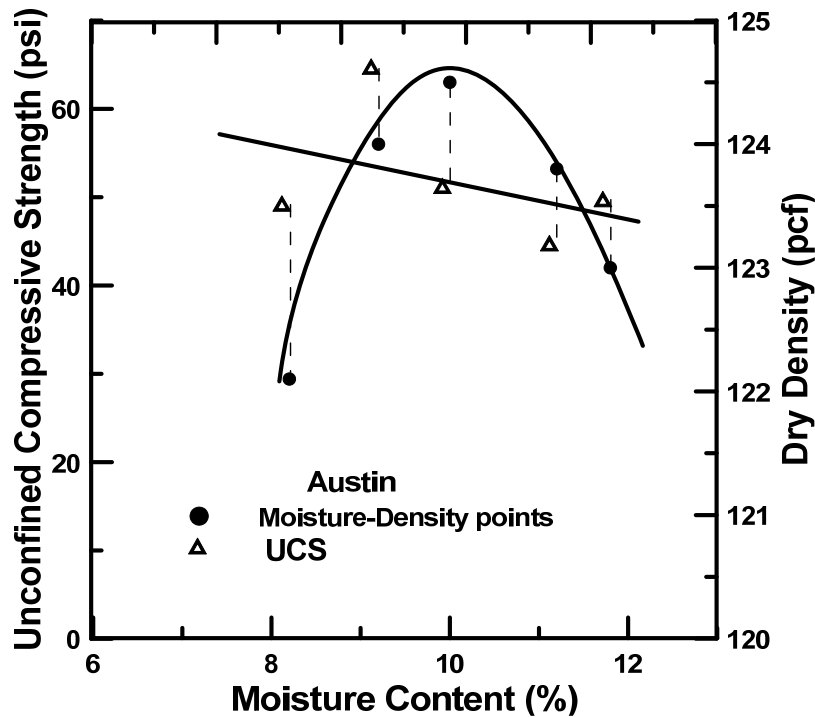


Figure 4.2 Unconfined Compressive Strength Results of Austin specimens

It can be noted from the above tables and figures that for El Paso soil, the highest unconfined compressive strength of 76 psi was observed at the sample test condition close to OMC-2% whereas for Austin soil, a higher unconfined compressive strength of 64.5 psi was observed at OMC-1% condition.

4.3 Soil Water Characteristic Curve (SWCC) Studies

Due to the presence of coarse material fraction in the soil specimens, some limitations were encountered in the determination of the SWCC. Tempe cell is typically used to obtain the SWCC of fine grained materials. The base materials have high coarse fraction, for example the El Paso base material has 7% of the material retained on the $7/8$ in. sieve. Since there are no universal

standards available to test these base materials, procedures similar to subgrades are followed for base material testing. Same Tempe cell was used to obtain the SWCC's of these unbound materials.

Samples of 2.5 in. diameter and 1 in. thickness were prepared at three different moisture content and dry density conditions, one on the wet of the optimum (OMC+2%), one on the optimum moisture content (OMC) and one on the dry side of the optimum moisture condition (OMC-2%). Soil samples were prepared, saturated and then placed on the saturated ceramic disk. The ceramic disk used in this study has an air entry value of 500 kPa. Air pressures of 10, 50, 100, 200, 300 and 450 kPa were applied for SWCC measurements. At equilibration, the moisture contents were recorded and these results are used to establish SWCC profile.

In this research, the SWCCs are plotted with matric suction on the x-axis (in log scale) and gravimetric water content was recorded on the y-axis. The SWCCs of El Paso and Austin base materials are shown in Figures 4.3 and 4.4, respectively.

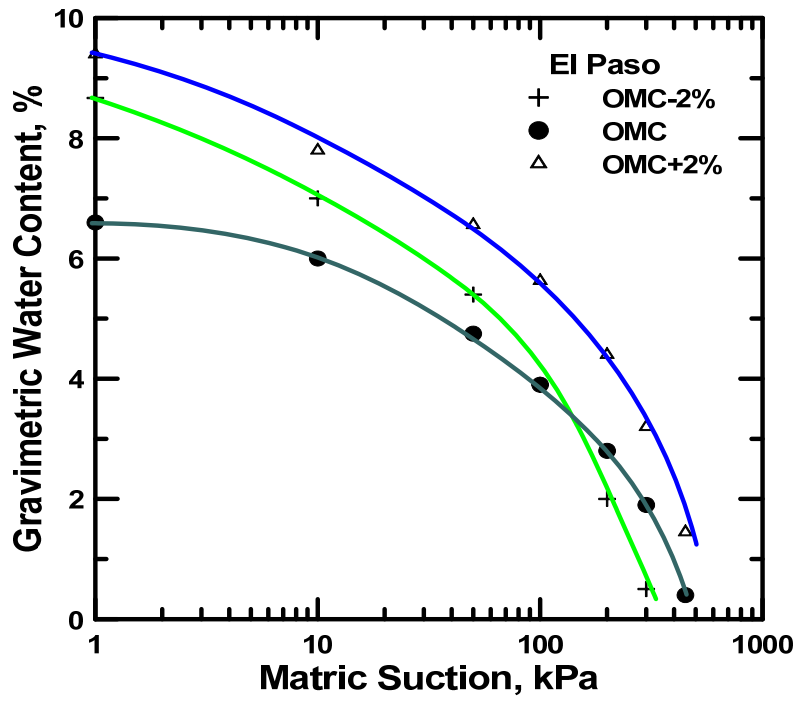


Figure 4.3 SWCC of El Paso specimens

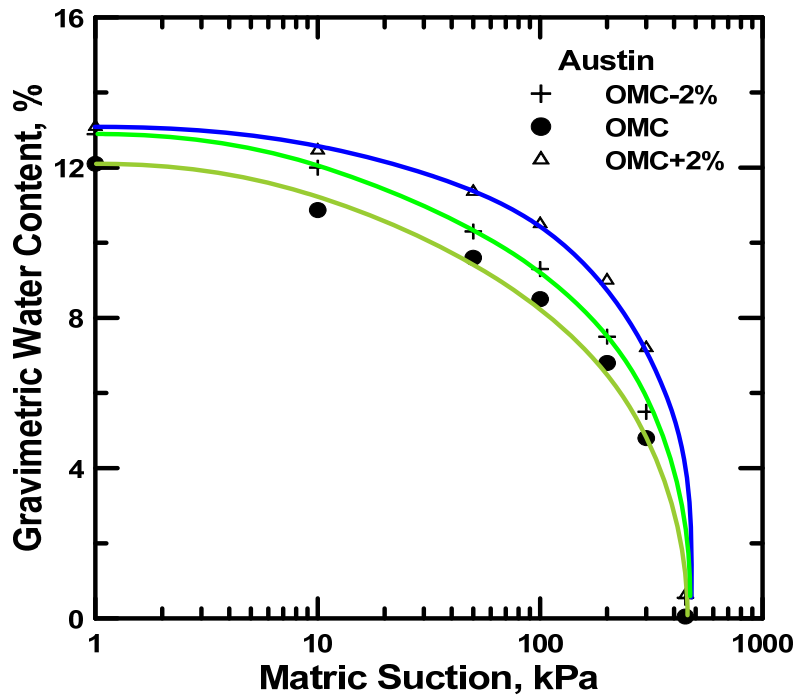


Figure 4.4 SWCC of Austin specimens

From the above figures, it can be mentioned that the air entry values of the soil samples compacted at OMC+2% are relatively higher when compared to the samples compacted at OMC and OMC-2%. Samples compacted at OMC-2% have lesser air entry values when compared to the samples at OMC condition. Specimens compacted wet of the optimum start to desaturate at higher suctions when compared to specimens compacted at optimum and dry of optimum conditions.

4.4 Resilient Modulus Test Results

The AASHTO standard test procedure, T-307-99 was followed for the determination of resilient moduli of the aggregate specimens. The combinations of various deviatoric and confining stresses applied in the test sequence have been tabulated in Table 3.5 presented in Chapter 3. In each test sequence, the specimen was subjected to five different confining stresses with three levels of deviatoric stresses applied at each confinement. A haversine loading wave with a frequency of 10 Hz was used to simulate the traffic wheel loading. Each loading cycle subjects the specimen to 0.1 sec of deviatoric or repeated loading and 0.9 sec of relaxation.

During the test, the average total vertical deformation was monitored and recorded using two external linear variable displacement transducers (LVDTs) placed on top of the triaxial cell. The internal load cell transducer placed inside the triaxial chamber recorded the deviatoric stress applied to the soil specimen.

Specimens molded at five different moisture content and dry density conditions (OMC-2%, OMC-1%, OMC, OMC+1%, OMC+2%) were subjected to resilient modulus testing under controlled suction conditions (First approach, as explained in chapter 3). Test specimens were saturated first and then placed carefully on the pedestal of the triaxial cell. The pedestal housed a ceramic disk with an air entry value of 1500 kPa. A membrane was tightened to the top and the bottom pedestals using o-rings. Then the triaxial chamber was assembled and the LVDTs were clamped on the top of the chamber for displacement measurements. Both air pressure and water lines were connected before the equilibration process.

As stated before, the moisture content of the specimen was varied by applying the desired matric suction. Under each air pressure applied, the specimens were expected to expel water until the equilibrium stage was reached. The equilibrium stage was reached only when the water stopped moving out from the soil specimen. The equilibration process expected to last a few days in the present base material testing since base materials contain fine materials.

In this study, El Paso soil specimen, compacted at OMC condition, was used in the suction controlled resilient modulus testing. The specimen was saturated first and was then placed inside the chamber. An air pressure of 50 kPa was applied and two water lines from the chamber were connected to the water columns of the Tempe cell. During the equilibration process, the water

column heights were monitored. Figure 4.5 provides the saturation process and unsaturated equipment used in this study.

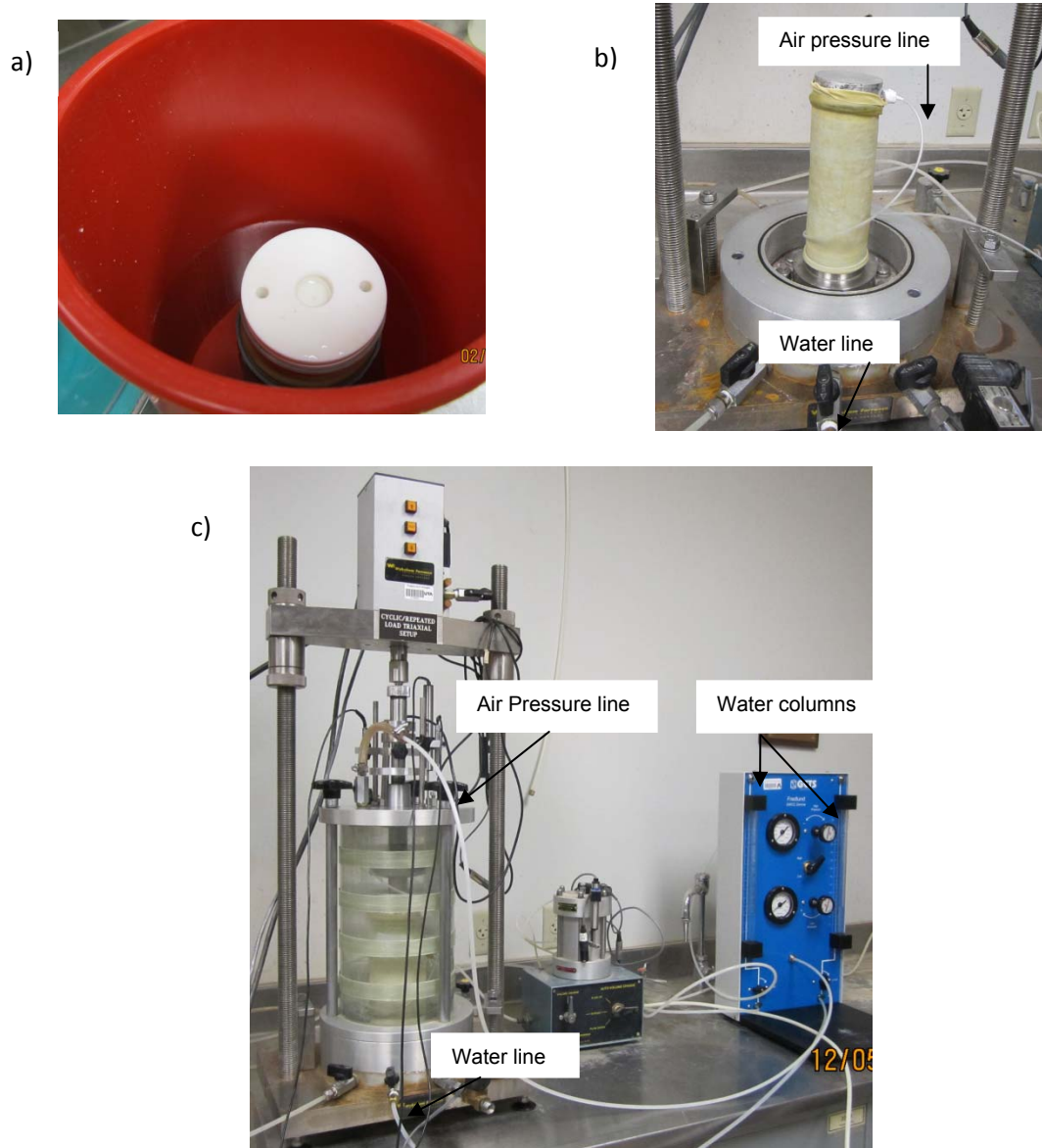


Figure 4.5 a) Saturating the specimen b) Specimen placed on the bottom pedestal c) Unsaturated equipment used in the study

As mentioned, the suction controlled resilient modulus test was planned to perform at two confining pressures with five relative deviatoric loading. Figure 4.6

show the M_R results versus deviatoric stress for net confining pressures of 35 kPa and 70 kPa of the El Paso specimen compacted at OMC at a matric suction value of 50 kPa.

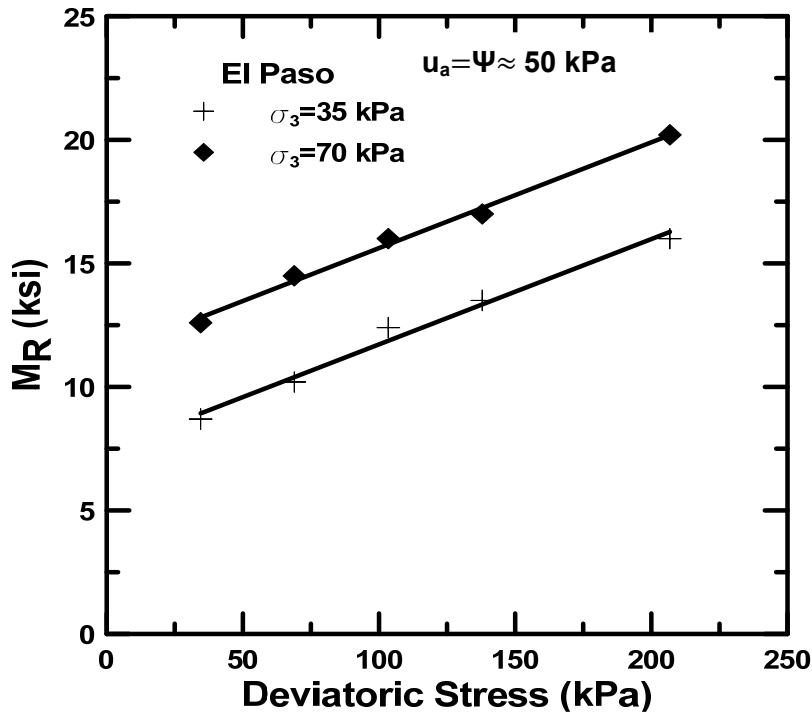


Figure 4.6 Suction Controlled M_R results of El Paso (OMC) specimen

The equilibration period for the El Paso soil specimen was longer than expected time duration. The time period to equilibrate was nearly a month and was mainly attributed to the finer fraction. It was also observed that while there were no changes in the water column heights in the burettes of the Tempe cell. This explains that the suction controlled testing is perhaps not needed as the applied deviatoric loading was small when compared to soil strength and hence did not result in any moisture imbalance during the testing. This means the

sample prepared at specific moisture content levels will not undergo any major moisture content changes during repeated loading.

As a result, the rest of the resilient modulus testing was conducted at various compacted moisture contents as per the second approach (moisture controlled M_R testing) outlined in Chapter 3. Moisture readings were monitored before and after the M_R testing and the results showed no appreciable differences.

Also, in the second approach, the soil specimens were compacted as per Table 3.4. The initial soil suction condition was established based on the SWCC information and the initial compaction moisture conditions. The prepared specimen with known suction value was placed on the ceramic disk. Two water lines from the pedestal which are connected to specimen were connected to the two water columns of the Tempe cell. During loading sequences, the water columns of the Tempe cell were monitored for any volume changes in the specimen.

Figure 4.7 shows comparisons between resilient moduli measured from suction controlled testing (1st approach) and moisture controlled testing (2nd approach) methods for the same net confining and deviatoric stresses. It can be noticed from the Figure 4.7 that resilient moduli results of the specimen compacted at OMC (tested as per 1st approach) are very close to the results of the specimens compacted at OMC (tested as per 2nd approach). Again, the

closeness of these results indicates that the present T-307 is probably sufficient for resilient modulus testing of base materials.

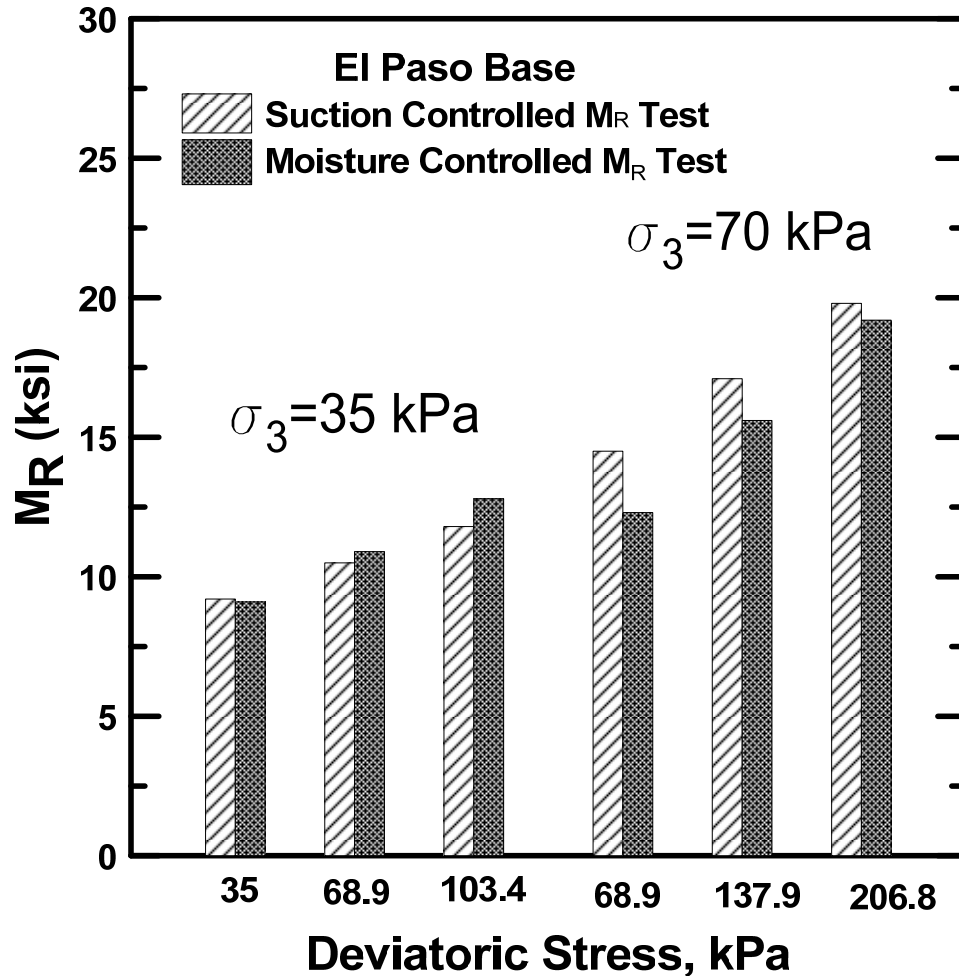
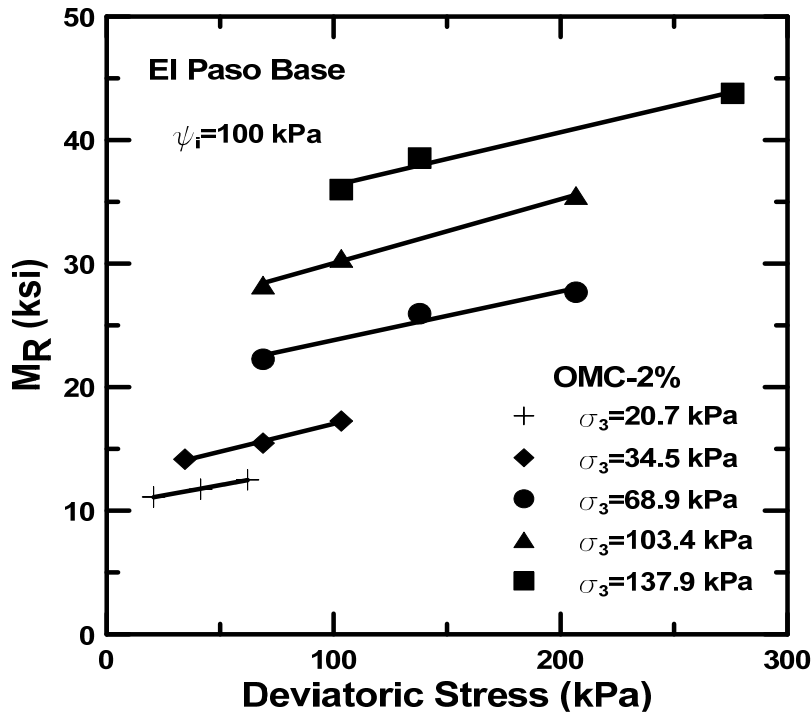
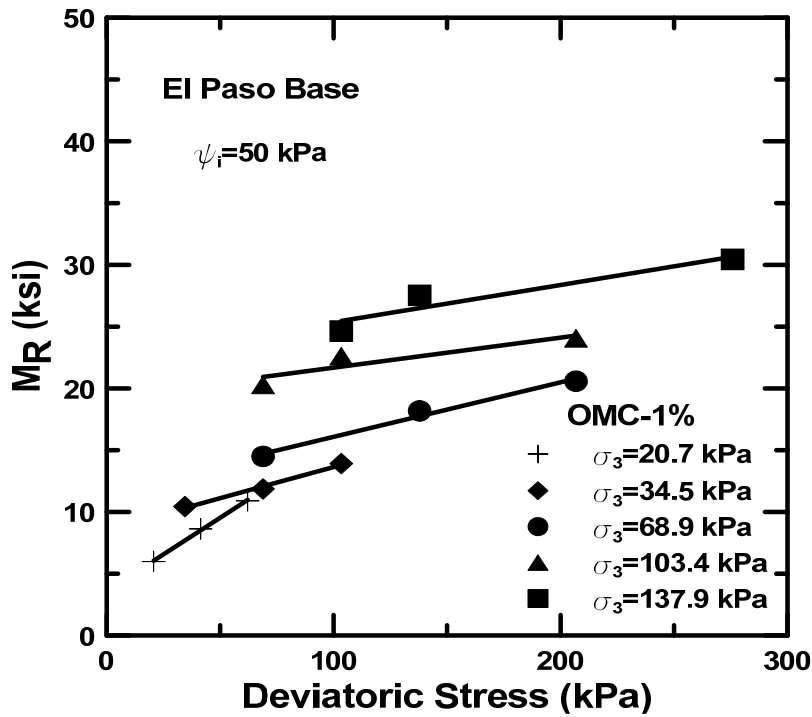


Figure 4.7 Comparison between M_R results from 1st and 2nd approach

To study the effect of variation of dry density and water content on resilient modulus results, samples were compacted at five different moisture content and dry density conditions. The laboratory results obtained for specimens compacted at different moisture content and dry densities are shown in the following Figures 4.8 through 4.12. The measured resilient modulus of El Paso and Austin specimens are plotted as a function of deviatoric and confining pressures.

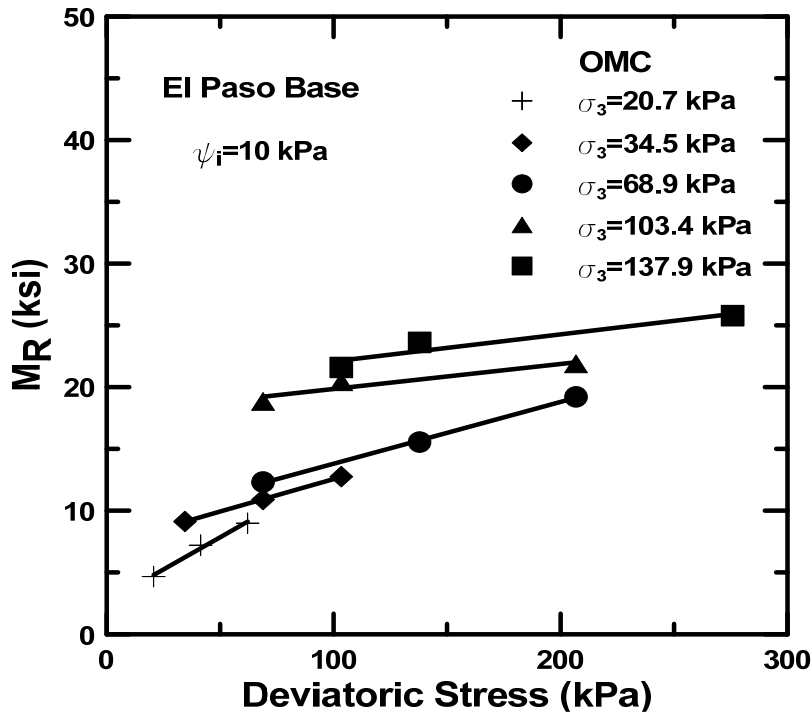


(a)

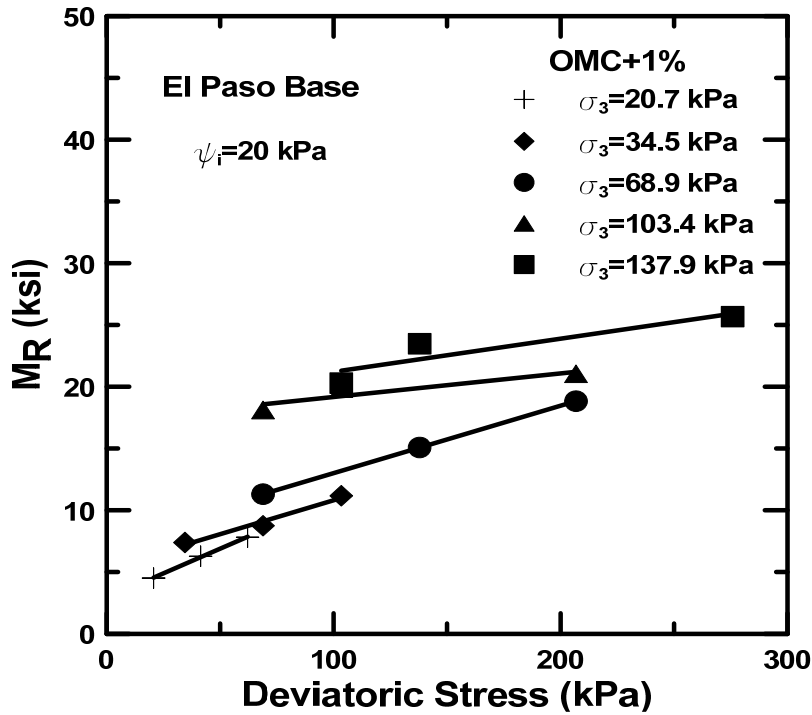


(b)

Figure 4.8 Variation of resilient modulus (M_R) of El Paso specimens compacted at (a) OMC-2%, and (b) OMC-1%

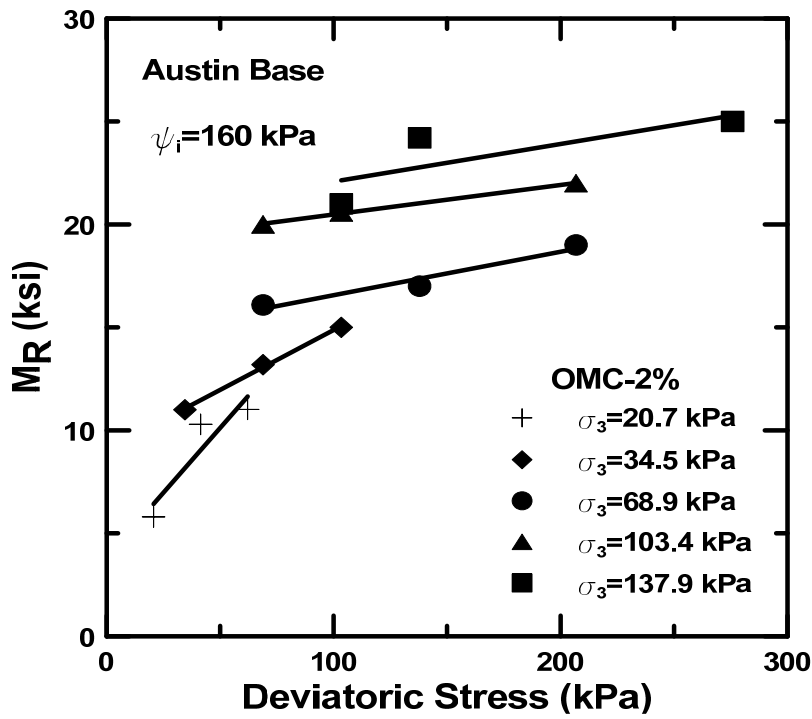


(a)

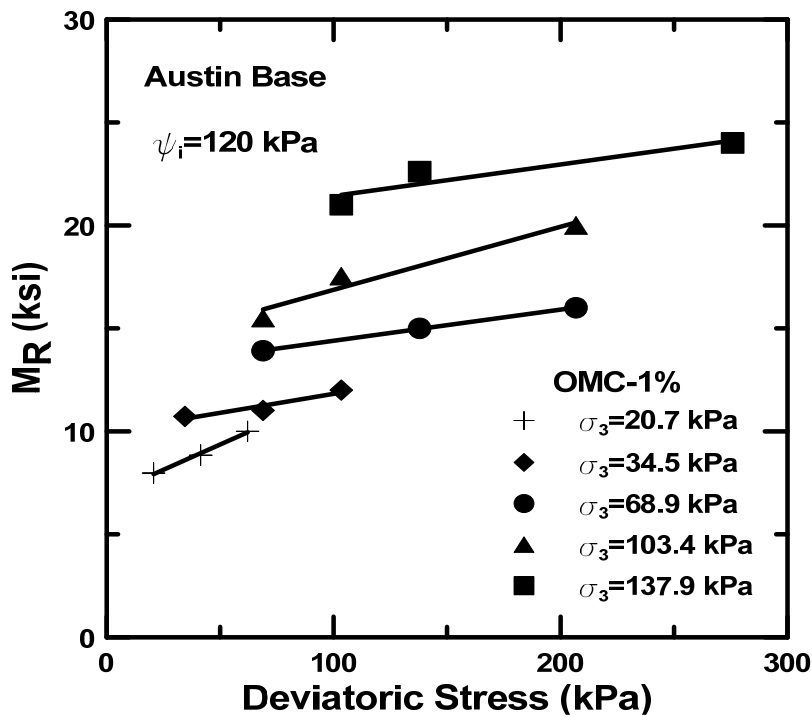


(b)

Figure 4.9 Variation of resilient modulus (M_R) of El Paso specimens compacted at (a) OMC, and (b) OMC+1%

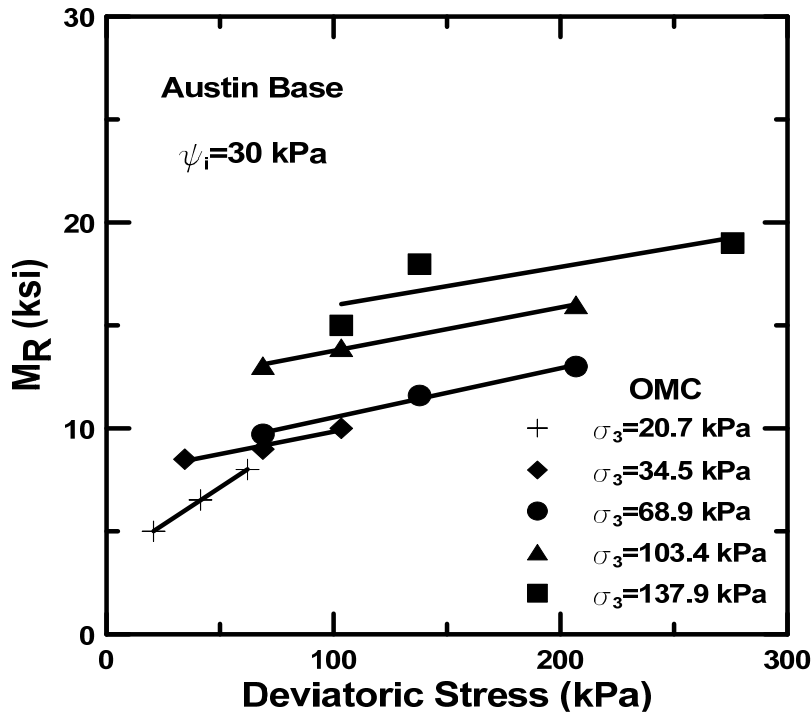


(a)

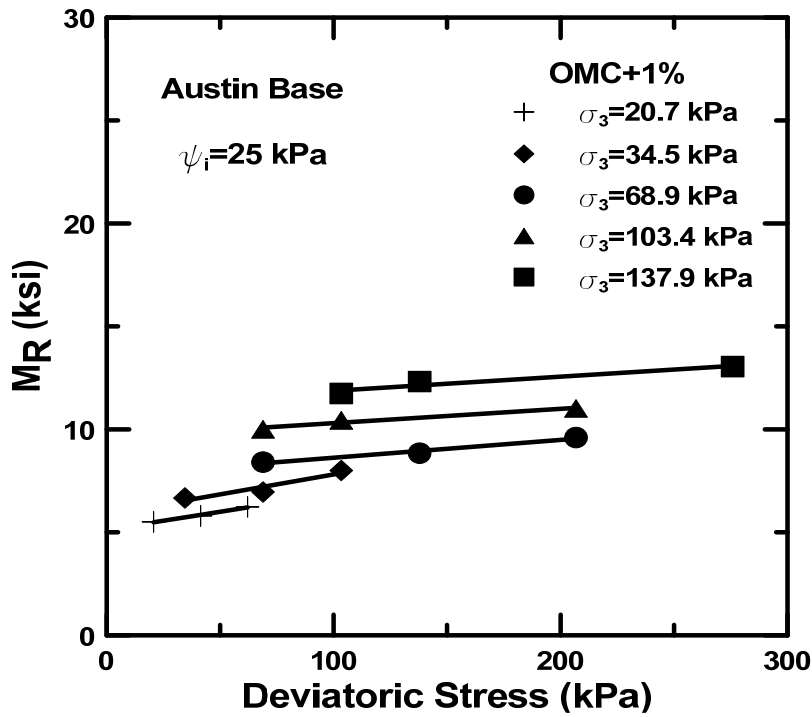


(b)

Figure 4.10 Variation of resilient modulus (M_R) of Austin specimens compacted at (a) OMC-2%, and (b) OMC-1%



(a)



(b)

Figure 4.11 Variation of resilient modulus (M_R) of Austin specimens compacted at (c) OMC, and (d) OMC+1%

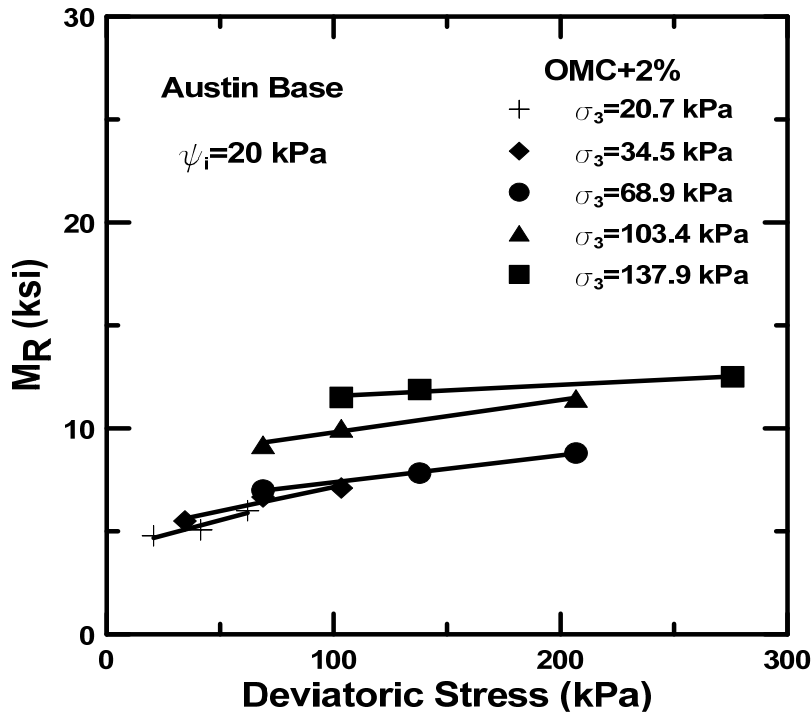


Figure 4.12 Variation of resilient modulus (M_R) of Austin specimen compacted at OMC+2%

It can be observed that both confining and deviatoric stresses have significant effect on the resilient modulus values of both base materials. With an increase in the deviatoric stress, the modulus of the material increased due to stress hardening of the coarse natured soil specimens. This behavior could be attributed to the fact that at higher confining pressure, the specimen has provided enough support from the surroundings when compared to lower confining pressures. In all the above cases, samples compacted at OMC-2% samples showed higher resilient modulus values than any other sample. Samples compacted on the wet side of OMC (OMC+2%) have lower resilient modulus values. A trend for samples compacted on dry side to exhibit higher M_R that wet

of optimum samples is observed because generally higher soil suction in dry of optimum samples than wet of optimum samples.

4.5 Modeling Analysis

4.5.1 *SWCC modeling and comparisons*

In this section, the SWCC predictions from MEPDG model were fully evaluated. The formulation was predicted using Fredlund and Xing (1994) equation. The recommended approach to characterize parameters of the SWCC from the soil properties is provided in the guide for Mechanistic-Empirical Pavement Design (NCHRP, 2004). As per MEPDG (NCHRP, 2004) three input levels are recommended to characterize the parameters of SWCC. Level 2 and prediction parameters are used to predict the SWCCs in this study and these predictions are compared with the measured SWCC from Tempe cell.

MEPDG SWCC Prediction Methodology Steps:

The basic input parameter needed from laboratory testing for Level 2

1. Optimum gravimetric water content (w_{opt}) and maximum dry unit weight (γ_{dmax})
2. Specific gravity of the solids (G_s)
3. Passing #200 sieve, effective grain size corresponding to 60 percent passing by weight (D_{60}) and Plasticity Index

Using these input variables, the SWCC model parameters such as a_f , b_f , c_f , and h_r are computed. The following steps show the procedure to obtain the

SWCC parameters and then these parameters are used with the Fredlund and Xing model to predict the SWCC of the soil.

1. Calculate $P_{200} \cdot PI$
2. Estimation of S_{opt} , θ_{opt} and θ_{sat} : These parameters are calculated using Y_{dmax} , w_{opt} and G_s using the equations given below:

$$\bullet \quad \theta_{opt} = \frac{w_{opt} Y_{dmax}}{\gamma_{water}} \quad (4-3)$$

$$\bullet \quad S_{opt} = \frac{\theta_{opt}}{1 - \frac{Y_{dmax}}{\gamma_{water} G_s}} \quad (4-4)$$

$$\bullet \quad \theta_{sat} = \frac{\theta_{opt}}{S_{opt}} \quad (4-5)$$

3. Determine the SWCC model parameters a_f , b_f , c_f , and h_r by using correlations with P_{200} , PI and D_{60}

3.1 If $(P_{200})(PI) > 0$

$$a_f = \frac{0.00364 (P_{200} PI)^{3.35} + 4 (P_{200} PI) + 11}{6.895}, \text{psi} \quad (4-6)$$

$$\frac{b_f}{c_f} = -2.313 (P_{200} PI)^{0.14} + 5 \quad (4-7)$$

$$c_f = 0.0514 (P_{200} PI)^{0.465} + 0.5 \quad (4-8)$$

$$\frac{h_r}{a_f} = 32.44 e^{0.0186(P_{200} PI)} \quad (4-9)$$

3.2 If $(P_{200})(PI) = 0$

$$a_f = \frac{0.8627(D_{60})^{-0.751}}{6.895}, \text{psi} \quad (4-10)$$

$$b_f = 7.5 \quad (4-11)$$

$$c_f = 0.1772 \ln(D_{60}) + 0.7734 \quad (4-12)$$

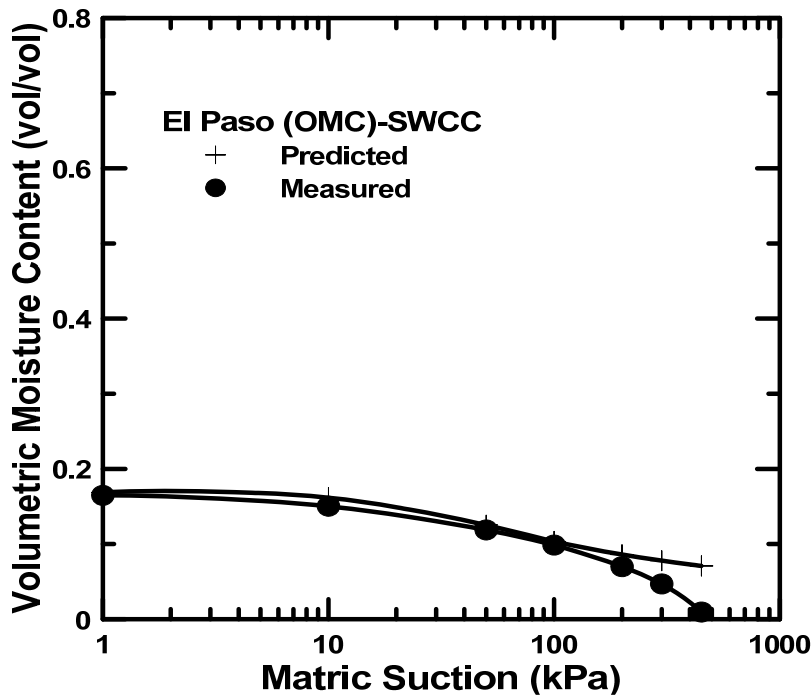
$$\frac{h_r}{a_f} = \frac{1}{D_{60} + 9.7 e^{-4}} \quad (4-13)$$

4. The SWCC will then be established using the Fredlund and Xing equation:

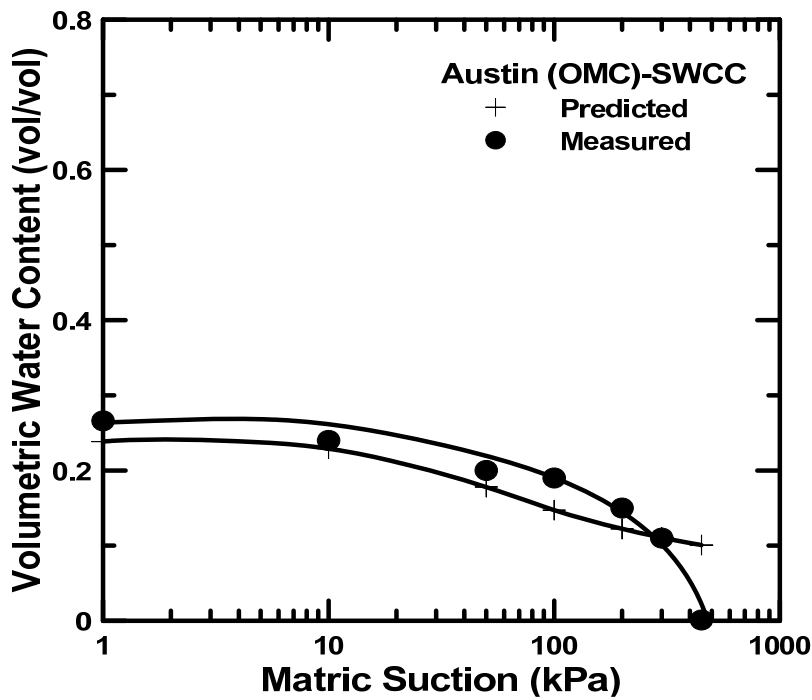
$$\theta_w = C(h) \times \left[\frac{\theta_{sat}}{\left[\ln \left[\text{EXP}(1) + \left(\frac{h}{a_f} \right)^{b_f} \right] \right]^{c_f}} \right] \quad (4-14)$$

$$C(h) = \left[1 - \frac{\ln \left[1 + \frac{h}{h_r} \right]}{\ln \left[1 + \frac{1.45 \times 10^5}{h_r} \right]} \right] \quad (4-14)$$

The above steps are followed to determine the SWCCs of El Paso and Austin base materials. These results are compared with the measured SWCC profiles. Figures 4.13 (a) and (b) show the comparisons between measured SWCC versus predicted SWCC of El Paso and Austin soils. Comparisons were made at optimum moisture content condition.



(a)



(b)

Figure 4.13 Predicted vs Measured SWCC (a) El Paso (b) Austin

The predicted values of volumetric water content obtained from Fredlund and Xing's (1994) model were compared with the experimental volumetric water contents. It can be observed that at higher suction, predicted results didn't match with the measured results. However, at low suctions, predicted results are well matched with the measured results. Overall, it is still preferable to use SWCCs from measurements as this curve has a paramount influence on the MEPDG design of pavements.

4.5.2 Resilient Modulus Models

4.5.2.1 Modified Universal Model

The data obtained from the testing program was filtered and then the Modified Universal Model expressed in Equation (4-1) was used to obtain the regression coefficients k_1 , k_2 and k_3 for each specimen.

$$M_R = k_1 \times p_a \times \left(\frac{\theta}{p_a} + 1\right)^{k_2} \times \left(\frac{\tau_{oct}}{p_a} + 1\right)^{k_3} \quad (4-1)$$

where, M_R = resilient modulus; p_a = atmospheric pressure; k_1 , k_2 , k_3 = regression constants; θ = bulk stress; τ_{oct} = octahedral shear stress.

The samples are tested at 15 different stress states. θ , τ_{oct} , and M_R are calculated from the test data. Using the above model (4-1), the regression constants k_1 , k_2 , k_3 are determined for each specimen. A non-linear regression analysis procedure included in a statistical software package called ProStat was used for this portion of the work. The regression coefficients of El Paso soil sample OMC which was tested under control suction testing are tabulated in

Table 4.3. The regression coefficients of El Paso and Austin samples which are tested as per second approach are tabulated in Table 4.4 and 4.5 respectively.

Table 4.3 Regression coefficients of El Paso soil (Suction Controlled Testing)

| Sample ID | | w % | Y_d (pcf) | Ψ (kPa) | w_i | w_f | k_1 | k_2 | k_3 | R^2 | M_R^* (ksi) |
|-----------|-----|-----|----------------|-----------------|-------|-------|-------|-------|-------|-------|------------------|
| 1 | OMC | 6 | 147 | ≈ 50 | 6.7 | 5.2 | 263 | 1 | 0 | 0.95 | 13.5 |

M_R^* - M_R representative at $\Theta = 31$ psi and $\tau_{oct} = 7$ psi

Table 4.4 Regression coefficients of El Paso soil (Moisture Controlled Testing)

| Sample ID | | w % | Y_d (pcf) | k_1 | k_2 | k_3 | R^2 | M_R^* (ksi) | Ψ (kPa) |
|-----------|--------|-----|----------------|-------|-------|-------|-------|------------------|-----------------|
| 1 | OMC-2% | 4 | 142 | 389 | 1.04 | -0.2 | 0.99 | 17.3 | 100 |
| 2 | OMC-1% | 5 | 145 | 288 | 0.98 | -0.01 | 0.96 | 13.9 | 50 |
| 3 | OMC | 6 | 147 | 234 | 1.03 | -0.01 | 0.94 | 12.8 | 10 |
| 4 | OMC+1% | 7 | 145 | 191 | 1.1 | 0 | 0.97 | 11.2 | 20 |
| 5 | OMC+2% | 8 | 142 | - | - | - | - | - | <5 |

M_R^* - Measured M_R representative at $\Theta = 31$ psi and $\tau_{oct} = 7$ psi

The OMC+2% sample of El Paso base material was too wet to test. The sample reached its 5% permanent deformation while loading. The suction of each sample was calculated from the SWCC curve.

Table 4.5 Regression coefficients of Austin soil (Moisture Controlled Testing)

| Sample ID | | w % | Y_d (pcf) | k_1 | k_2 | k_3 | R^2 | M_R^* (ksi) | Ψ (kPa) |
|-----------|--------|-----|----------------|-------|-------|-------|-------|------------------|-----------------|
| 1 | OMC-2% | 8 | 122 | 349 | 0.92 | -0.34 | 0.9 | 13.6 | 160 |
| 2 | OMC-1% | 9 | 124 | 340 | 0.88 | -0.39 | 0.98 | 11.6 | 120 |
| 3 | OMC | 10 | 125 | 269 | 0.8 | -0.12 | 0.97 | 9.6 | 30 |
| 4 | OMC+1% | 11 | 124 | 251 | 0.71 | -0.27 | 0.99 | 7.4 | 25 |
| 5 | OMC+2% | 12 | 122 | 209 | 0.79 | -0.32 | 0.97 | 7.1 | 20 |

M_R^* - Measured M_R representative at $\Theta = 31$ psi and $\tau_{oct} = 7$ psi

From the above two Tables 4.4 and 4.5, it can be concluded that as the water content decreased, the resilient modulus value increased. As anticipated, the maximum modulus occurred at moisture dry of optimum moisture content (OMC-2%). The quality of the data collected was good, and the fitted models described the collected data well as judged by the R^2 values in excess of 0.9. Figure 4.14 presents the variation of resilient modulus with respect to matric suction.

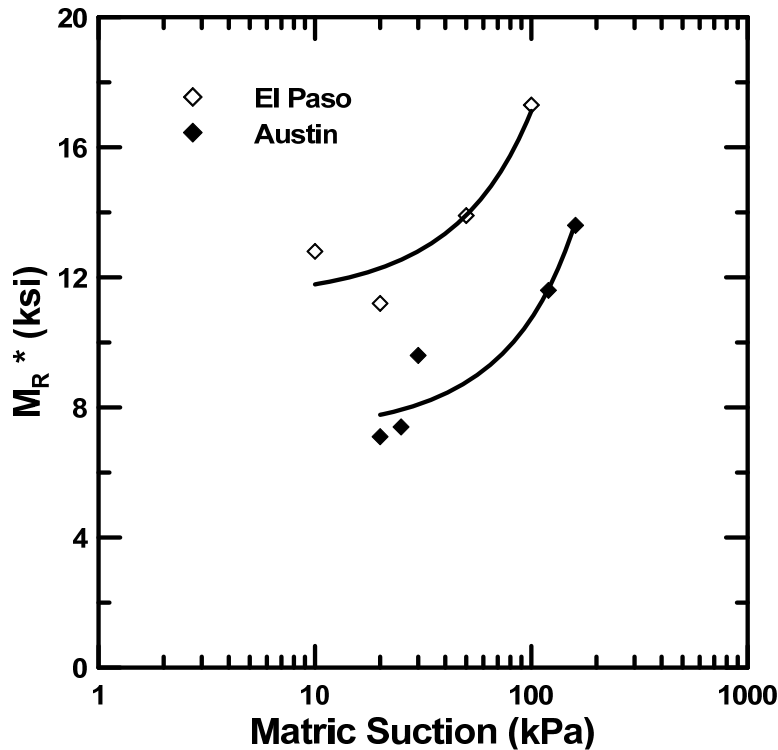
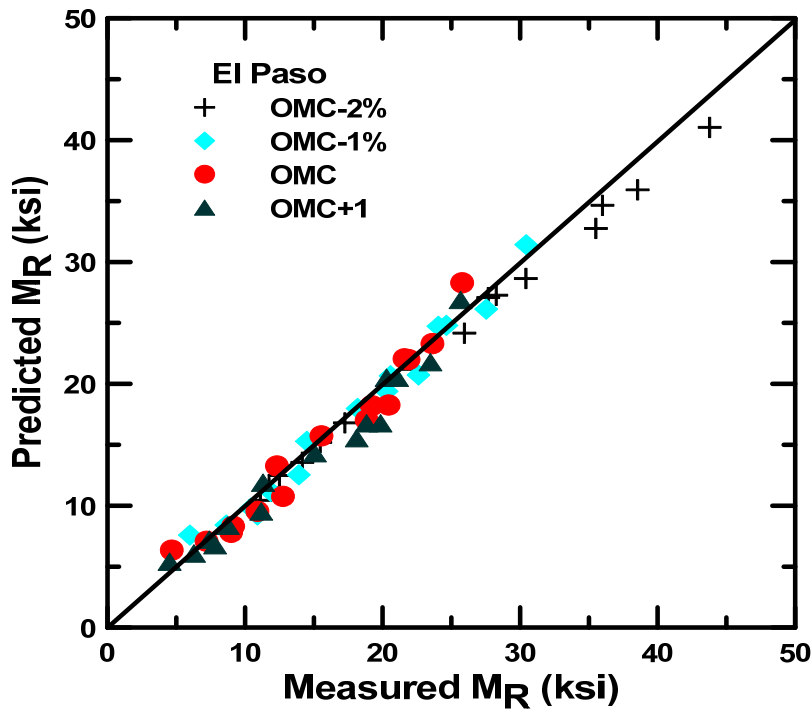


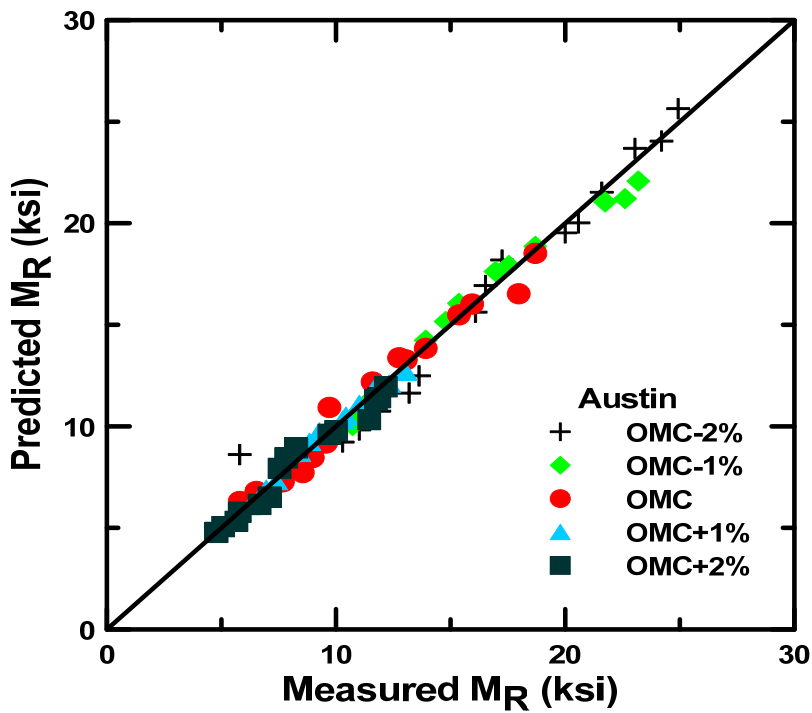
Figure 4.14 M_R - Matric Suction relationship

Resilient modulus variation with respect to matric suction is nonlinear for all the specimens tested. In general, M_R increases with increase in matric suction. In this study, the samples are compacted at different densities which indicate inconsistency in the matric suction values. For example, El Paso sample compacted at OMC has less matric suction than the sample compacted at OMC+1%. This inconsistency is because both the samples are compacted at two different densities.

Using the nonlinear parameters k_1 , k_2 , and k_3 , the resilient modulus (M_R) values were back calculated and these results are compared by plotting predicted M_R on Y axis and measured M_R on x axis. Figures 4.15 (a) and (b) show M_R comparisons of El Paso and Austin soils.



(a)



(b)

Figure 4.15 Predicted vs Measured M_R results (Universal model)
 (a) El Paso specimens (b) Austin specimens

From the Figures 4.15 (a) and (b), it can be noted that resilient modulus values of El Paso and Austin specimens have a best fit to the modified universal model. The predicted resilient moduli are nearly the same as the measured results for both El Paso and Austin specimens.

Another suction based model was used in the following analysis. The results are discussed in the following.

4.5.2.2 Cary and Zapata model

As previously discussed in chapter 2, various research studies have been conducted to predict M_R values. In addition, most of the models are based on regression analysis on specific types of soils. In this study, revised model of Cary and Zapata (2010) was used to predict the M_R values. This model was proposed for both fine- and coarse- grained materials in terms of particle size and plasticity of the materials:

$$\log\left(\frac{M_R}{M_{R-opt}}\right) = (\alpha + \beta \times e^{-wPI})^{-1} + \frac{(\delta + \gamma \times wPI^{0.5}) - (\alpha + \beta \times e^{-wPI})^{-1}}{1 + e^{\left(\ln\left(\frac{-(\delta + \gamma \times wPI^{0.5})}{(\alpha + \beta \times e^{-wPI})^{-1}}\right) + (\rho + \omega \times e^{-wPI})^{0.5} \times \left(\frac{S - S_{opt}}{100}\right)\right)}} \quad (4-2)$$

Where M_R = resilient modulus at a given time and moisture level,

M_{R-opt} = resilient modulus at optimum moisture content,

wPI = water content at Plasticity Index,

S = degree of saturation corresponding to M_R ,

S_{opt} = optimum degree of saturation corresponding to M_{Ropt} , and

$\alpha, \beta, \delta, \gamma, \rho, \omega$ = model fitting parameters as function of soil type and gradation

Based on the previous studies and results, Cary and Zapata (2010) concluded the model fitting parameters as

$$\alpha = -0.6, \beta = -1.87194, \delta = 0.8, \gamma = 0.08, \rho = 11.96518, \text{ and } \omega = -10.19111$$

Using these model parameters and results obtained from lab testing (w_{PI} , S , S_{opt} , and M_{R-opt}) resilient modulus M_R at any different moisture level (OMC-2%, OMC-1%, OMC+1%, and OMC+2%) are predicted. The following Tables 4.6 and 4.7 provide the measured and predicted resilient modulus results of both El Paso and Austin soil specimens. The predicted versus measured resilient modulus results are plotted in the following figures (Figure 4.16 (a) and (b)).

Table 4.6 Measured vs Predicted M_R results of El Paso specimens

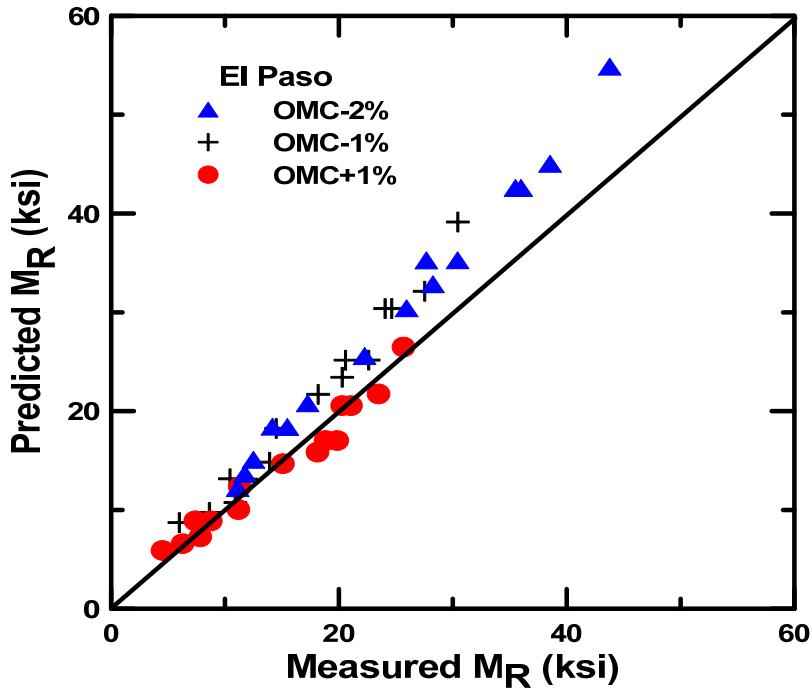
| σ_3 (kPa) | σ_d (kPa) | M_{R-opt} MPa (ksi) | Resilient Modulus M_R , MPa (ksi) | | | | | |
|---------------------|---------------------|-----------------------------|-------------------------------------|-------------|-------------|-------------|-------------|-------------|
| | | | OMC-2% | | OMC-1% | | OMC+1% | |
| | | | M | P | M | P | M | P |
| 20.7 | 20.7 | 43 (6) | 77 (11) | 84 (12) | 41 (6) | 60 (9) | 31 (5) | 41 (6) |
| | 41.4 | 48 (7) | 81 (12) | 94 (14) | 60 (9) | 67 (10) | 43 (6) | 46 (7) |
| | 62.1 | 53 (8) | 86 (12) | 104 (15) | 75 (11) | 74 (11) | 54 (8) | 50 (7) |
| 34.5 | 34.5 | 65 (9) | 98 (14) | 127 (18) | 72 (10) | 91 (13) | 51 (7) | 61 (9) |
| | 68.9 | 65 (9) | 107 (15) | 127 (18) | 82 (12) | 91 (13) | 60 (9) | 61 (9) |
| | 103.4 | 74 (11) | 119 (17) | 144 (21) | 96 (14) | 102 (15) | 77 (11) | 69 (10) |
| 68.9 | 68.9 | 91 (13) | 154 (22) | 177 (26) | 100 (15) | 126 (18) | 78 (11) | 85 (12) |
| | 137.9 | 108 (16) | 178 (26) | 210 (30) | 125 (18) | 150 (22) | 104 (15) | 101 (15) |
| | 206.8 | 125 (18) | 191 (28) | 243 (35) | 142 (21) | 174 (25) | 130 (19) | 117 (17) |
| 103.4 | 68.9 | 116 (17) | 195 (28) | 227 (33) | 140 (20) | 162 (23) | 125 (18) | 109 (16) |
| | 103.4 | 125 (18) | 210 (30) | 243 (35) | 156 (23) | 174 (25) | 137 (20) | 117 (17) |
| | 206.8 | 151 (22) | 245 (36) | 294 (43) | 166 (24) | 210 (30) | 145 (21) | 142 (21) |
| 137.9 | 103.4 | 151 (22) | 248 (36) | 294 (43) | 170 (25) | 210 (30) | 140 (20) | 142 (21) |
| | 137.9 | 160 (23) | 266 (39) | 311 (45) | 190 (28) | 222 (32) | 162 (23) | 150 (22) |
| | 275.8 | 194 (28) | 302 (44) | 379 (55) | 210 (30) | 270 (39) | 177 (26) | 183 (26) |

M-measured & P-predicted

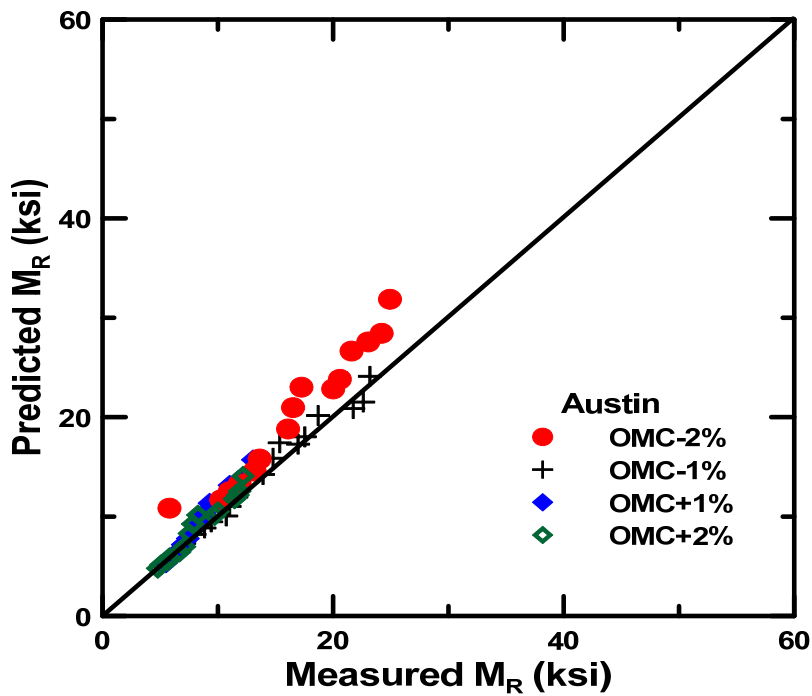
Table 4.7 Measured vs Predicted M_R results of Austin specimens

| σ_3 (kPa) | σ_d (kPa) | M_{R-opt} MPa (ksi) | Resilient Modulus M_R , MPa (ksi) | | | | | | | |
|---------------------|---------------------|-----------------------------|-------------------------------------|-------------|-------------|-------------|------------|-------------|------------|------------|
| | | | OMC-2% | | OMC-1% | | OMC+1% | | OMC+2% | |
| | | | M | P | M | P | M | P | M | P |
| 20.7 | 20.7 | 43 (6) | 40 (6) | 75 (11) | 55 (8) | 57 (8) | 38 (6) | 37 (5) | 33 (5) | 33 (5) |
| | 41.4 | 47 (7) | 71 (10) | 81 (12) | 61 (9) | 61 (9) | 40 (6) | 40 (6) | 35 (5) | 36 (5) |
| | 62.1 | 50 (7) | 76 (11) | 86 (13) | 65 (9) | 65 (9) | 43 (6) | 43 (6) | 39 (6) | 38 (6) |
| 34.5 | 34.5 | 53 (7) | 82 (12) | 92 (13) | 74 (11) | 69 (10) | 46 (7) | 45 (7) | 40 (6) | 41 (6) |
| | 68.9 | 58 (8) | 91 (13) | 101 (15) | 76 (11) | 76 (11) | 48 (7) | 50 (7) | 46 (7) | 44 (6) |
| | 103.4 | 63 (9) | 94 (14) | 109 (16) | 80 (12) | 83 (12) | 51 (7) | 54 (8) | 49 (7) | 48 (7) |
| 68.9 | 68.9 | 75 (11) | 111 (16) | 130 (19) | 96 (14) | 98 (14) | 58 (8) | 64 (9) | 52 (8) | 57 (8) |
| | 137.9 | 84 (12) | 114 (17) | 145 (21) | 102 (15) | 110 (16) | 61 (9) | 71 (10) | 54 (8) | 64 (9) |
| | 206.8 | 92 (13) | 119 (17) | 159 (23) | 106 (15) | 120 (17) | 64 (9) | 78 (11) | 57 (8) | 70 (10) |
| 103.4 | 68.9 | 92 (13) | 138 (20) | 158 (23) | 117 (17) | 119 (17) | 71 (10) | 78 (11) | 67 (10) | 70 (10) |
| | 103.4 | 95 (14) | 142 (21) | 164 (24) | 121 (18) | 124 (18) | 72 (10) | 81 (12) | 69 (10) | 73 (11) |
| | 206.8 | 107 (15) | 149 (22) | 184 (27) | 129 (19) | 139 (20) | 76 (11) | 91 (13) | 79 (11) | 81 (12) |
| 137.9 | 103.4 | 111 (16) | 159 (23) | 190 (28) | 150 (22) | 144 (21) | 81 (12) | 94 (14) | 81 (12) | 84 (12) |
| | 137.9 | 114 (17) | 167 (24) | 196 (28) | 156 (23) | 149 (22) | 85 (12) | 97 (14) | 82 (12) | 87 (13) |
| | 275.8 | 128 (19) | 172 (25) | 220 (32) | 160 (23) | 166 (24) | 90 (13) | 108 (16) | 84 (12) | 97 (14) |

M-measured & P-predicted



(a)



(b)

Figure 4.16 Predicted vs Measured M_R results (Cary and Zapata model)
 (a) El Paso specimens and (b) Austin specimens

From the Figures 4.16 (a) and (b), it can be noted that the measured resilient modulus results are well matched with the predicted results. The suction model proposed by Cary and Zapata are predicting higher for the specimens compacted on the dry side (OMC-1% and OMC-2%). Whereas the specimens compacted on the wet side are well matched with the predicted results for both the materials.

4.6 Summary

This chapter mainly discusses the advanced soil tests which include unconfined compressive strength, soil water characteristic curve and resilient moduli properties of El Paso and Austin base materials. Effect of confining pressure, deviatoric stress and matric suction on the resilient properties are explained. The final section covers the regression modeling analysis of the resilient moduli results using three parameter confining pressure and deviatoric stress model (Modified Universal model) and Cary and Zapata model. Also, the soil water characteristic curve predictions using MEPDG method was evaluated for the present base materials.

The next chapter summarizes all the different tests that were conducted in this research and conclusions were made based on these studies. Also, recommendations for future studies were provided.

CHAPTER 5

SUMMARY AND CONCLUSIONS

5.1 Summary

In this research, two base materials with different gradations were selected and studied. Basic tests such as sieve analysis, Atterberg limits, and modified proctor tests were first conducted. Tempe cell was used to obtain the soil water characteristic curve of the unbound materials at different compaction conditions. Advanced tests such as resilient modulus and unconfined compressive strength tests were performed at five select moisture content and dry density conditions. The second part comprises of analyzing the measured test data using universal and other models. Based on the experimental data and analyses performed, the following conclusions are drawn:

1. The higher unconfined compressive strength was observed for both bases on the dry side of the optimum condition. For El Paso soil, the highest unconfined compressive strength of 76 psi was observed at the test condition close to OMC-2% whereas for Austin soil, a higher unconfined compressive strength of 64.5 psi was observed at OMC-1% condition.
2. From the soil water characteristic curves, the air entry values of the soil samples compacted at OMC+2% are relatively higher when compared to the same soil samples compacted at OMC and OMC-2%. This is because

specimens compacted at wet of the optimum start to desaturate at higher suctions when compared to specimens compacted at optimum and dry of optimum conditions.

3. While testing suction controlled resilient modulus test, it was observed that there were no changes in the water column heights in the burettes of the Tempe cell, which indicate that moisture contents inside the soil specimens have not experienced any drainage. This is because the applied deviatoric loading was small when compared to soil strength and hence this did not result in appreciable volume changes or related moisture imbalance during the testing.
4. The resilient moduli results obtained from the suction controlled testing (1st approach) and the same from AASHTO T-307 (2nd approach) method are close to each other for the same stress state conditions. The closeness of these results indicates that the T-307 method is sufficient for resilient modulus testing of base materials and there is no need for performing suction controlled M_R testing on these materials.
5. The present moduli tests showed that both confining and deviatoric stresses have shown a major influence on the resilient moduli values of the base materials. An increase in the deviatoric stress resulted in an increase in the resilient modulus of the material, which is attributed to stress hardening of the aggregate specimen at high deviatoric stresses. This deviatoric stress effect on moduli is more pronounced at low

- confining pressures than at high confining pressures. This is because, at high confining pressures, the granular cemented specimen is strong and hence does not respond to increased axial deviatoric stresses as it does at low confining pressures.
6. From the soil water characteristic curve analysis, the Level 2 from MEPDG that is based on Fredlund and Xing's model predictions have provided SWCC predictions that are well matched with the measured data. A slight deviation in the trend was observed at higher suction.
 7. From the results obtained from resilient modulus analysis, it was noted that resilient modulus values of El Paso and Austin specimens have shown to be modeled well with the modified universal model. The suction model proposed by Cary and Zapata is also attempted and the back calculation from this model showed that the predicted M_R values are higher for the specimens compacted on the dry side (OMC-2% and OMC-1%). The specimens compacted on the wet side are well matched with the predicted M_R results for both the materials.

5.2 Recommendations for future research

Based on the experience gained from this study, some important recommendations are proposed.

1. The amount of testing and results obtained were not extensive enough and hence further testing on a broader range of soil types is recommended. Another important finding of this study is the limitations

encountered when trying to equilibrate a specimen under a fixed matric suction level, before starting the M_R test.

2. A simpler procedure should be established to lessen the time required for equilibration of suction in the sample.

REFERENCES

1. Abu-Farsakh, M., K. Alshibli, M. Nazzal, and E. Seyman., (2004) "Assessment of In Situ Test Technology for Construction Control of Base Course and Embankments". Final Report No. FHWA/LA.04/385, Louisiana Transportation Research Center, Baton Rouge.
2. Amber, Y., and Von Quintus, H. L., (2002). "Study of LTPP Laboratory Resilient Modulus Test Data and Response Characteristics". Final Report. FHWA-RD- 02-051, USDOT. FHWA.
3. Anderson, D.G., Woods, R.D. (1975) "Comparison of field and laboratory shear moduli". Proceedings, Conference on In situ Measurement of Soil Properties. Specialty Conference of the Geotechnical Engineering Division A.S.C.E., Raleigh, North Carolina, vol.1, pp.69-92.
4. Barksdale, R.D., J. Alba, P.N. Khosla, R. Kim, P.C. Lambe, and M.S. Rahman., (1997). "Laboratory Determination of Resilient Modulus for Flexible Pavement Design". NCHRP Web Document 14, Federal Highway Administration, Washington, D.C., 486 pp.
5. Cary, C.E. and Zapata, C.E., (2010), "Enhanced Model for Resilient Response of Soils Resulting from Seasonal Changes as Implemented in Mechanistic-Empirical Pavement Design Guide".

6. Choubane, B. and R.L. McNamara, (2000). "Flexible Pavement Embankment Moduli Using Falling Weight Deflectometer (FWD) Data". Research Report FL/DOT/SMO/00-442, State Materials Office, Florida Department of Transportation, Tallahassee.
7. Drumm, E. C., Reeves, J. S., Madgett, M. R., and Trolinger, W. D., (1997), "Subgrade Resilient Modulus Correction for Saturation Effects". Journal of Geotechnical and Geoenvironmental Engineering, Vol. 123, No. 7, pp. 663-670.
8. Edil, T., C. Benson, and A. Sawangsuriya, (2006). "Resilient Behavior of Unsaturated Subgrade Soils". Interim Report to University of Minnesota, University of Wisconsin–Madison.
9. Fredlund, D. G., and A.Xing (1994). "Equations for the Soil-Water Characteristic Curve". Canadian Geotechnical Journal, Vol. 31, No. 4, pp. 521 – 532.
10. Gupta, S., Ranaivoson, A., Edil, T., Benson, C., Sawangsuriya, A., (2007), "Pavement Design Using Unsaturated Soil Technology". Report No. MN/RC-2007-11, Final Research Report submitted to Minnesota Department of Transportation, University of Minnesota, Minneapolis.
11. Hopkins, T., Beckham, Tony. L., Sun, C., and Ni, B., (2004). "Resilient Modulus of Kentucky Soils". Final Research Report for Kentucky Transportation Cabinet, Kentucky Transportation Center, University of Kentucky.

12. Hopkins, T. C., Bekham, T.L., and Sun, C., (2007), "Resilient Modulus of Compacted Crushed Stone Aggregate Bases". Research report KTC-05-27/SPR-229-01-1F. Kentucky Transportation Center, University of Kentucky.
13. Hossain M. S., (2008), "Characterization of Subgrade Resilient Modulus for Virginia Soils and Its Correlation with the Results of Other Soil Tests". Final Report VTRC 09-R4, Virginia Transportation Research Council.
14. Hossain M.S. and Apegyei A.K., (2010), "Evaluation of the Lightweight Deflectometer for In-Situ Determination of Pavement Layer Moduli". Research Report VTRC 10-R6, Virginia Department of Transportation.
15. Khoury, N. N., and Zaman, M. M., (2004), "Correlation between Resilient Modulus, Moisture Variation, and Soil Suction for Subgrade Soils". Transportation Research Record: Journal of Transportation Research Board 1874, National Research Council, Washington, D.C., pp. 99-107.
16. Leong, E.C., and H. Rahardjo (1996). "A Review on Soil-Water Characteristic Curve Equations". Geotechnical Research Report, NTU/GT/96-5, Nanyang Technological University, NTU-PWD Geotechnical Research Center, Singapore.
17. Malla, R. B., and Joshi, S., (2006), "Establishing Subgrade Support Values for Typical Soils in New England". Report No. NETCR 57, New England Transportation Consortium, Fall River, Mass.
18. McCartney, J.S., Selvam, R.P., King, J., and Khosravi, A., (2010), "Evaluation of the enhanced integrated climatic model for the Arkansas State Highway

and Transportation Department”. Research Report, University of Arkansas-Fayetteville.

19. Mohammad, L.N., B. Huang, A.J. Puppala, and A. Allen., (1999) “Regression Model for Resilient Modulus of Subgrade Soil”. Transportation Research Record 1687, Transportation Research Board Record, National Research Council, Washington, D.C., pp. 47–54.
20. Mohammad, L. N., Puppala, A. J., and Alavilli, P., (1994a), “Influence of Testing Procedure and LVDTs Location on Resilient Modulus of Soils”. Transportation Research Record 1462, Transportation Research Board, National Research Council, Washington, D.C., pp. 91-101.
21. Mohammad, L. N., Puppala, A. J., and Alavilli, P., (1994b), “Investigation of the Use of Resilient Modulus for Louisiana Soils in Design of Pavements”. Final Report No. 283, Louisiana Transportation Research Center, Federal Highway Administration, Louisiana Department of Transportation and Development.
22. Mooney M.A., Rinehart R.V., Facas N.W., Musimbi, O.M., White D.J. and Vennapusa P.K.R. (2010), “Intelligent Soil Compaction Systems,” NCHRP Report 676, Transportation Research Board, Washington, DC, 178 p.
23. Nazarian, S., Pezo, R., (1996), “An Approach to Relate Laboratory and Field Moduli of Base Materials.” Report No. 1336-2F, Texas Department of Transportation in cooperation with Federal Highway Administration, Texas.

24. Nazarian, S., Yuan, D., (2008), "Variation in Moduli of Base and Subgrade with Moisture." ASCE Geotechnical Special Publication. Volume 178. Page(s) 570-577.
25. Nelson, C.R., D.L. Petersen, R.L. Peterson, J.C. Rudd, and E. Sellman, (2004) "Design and Compaction Control for Foundation Soil Improvements." T.H. 61 Reconstruction, New Port, Minnesota (CD-ROM), Presented at the 83rd Annual Meeting of the Transportation Research Board, Washington, D.C.
26. Newcomb, D.E. and B. Birgisson., (1999). "NCHRP Synthesis of Highway Practice 278: Measuring In-Situ Mechanical Properties of Pavement Subgrade Soils". Transportation Research Board, National Research Council, Washington, D.C.
27. Ooi, P. S. K., Sandefur, K. G., and Archilla, A. R., (2006), "Correlation of Resilient Modulus of Fine-Grained Soils with Common Soil Parameters for Use in Design of Flexible Pavements," Report No. HWY-L-2000-06, Hawaii Department of Transportation, Honolulu.
28. Pacheco L.G., (2010), "Impact of Moisture Content and Density Variations on Time Dependent Strength and Modulus of Compacted Geomaterials." MS Thesis, University of Texas at El Paso, El Paso, Texas.
29. Pacheco, L.G., Nazarian, S., (2011), "Impact of Moisture Content and Density on Stiffness-Based Acceptance of Geomaterials," In Journal of Transportation Research Board 90th

30. Pedarla, A. (2008). "Durability studies on stabilization effectiveness of soils containing different fractions of montmorillonite", Thesis submitted to the department of civil engineering, The University of Texas at Arlington, Texas in partial fulfillment of the master degree.
31. Potturi, A. K. (2006). "Evaluation of resilient modulus of cement and cement-fiber treated reclaimed asphalt pavement aggregates using repeated load triaxial test", Thesis submitted to the the department of civil engineering, The University of Texas at Arlington, Texas in partial fulfillment of the master degree.
32. Puppala, A.J., (2008), "Estimating Stiffness of Subgrade and Unbound Materials for Pavement Design," NCHRP Synthesis 382, Transportation Research Board, Washington, DC, 129 p.
33. Puppala, A.J., Thammanoon, M., Nazarian, S., Hoyos, L.R., and Chittoori, B. (2012), "Insitu matric suction and moisture content measurements in expansive s clay during seasonal fluctuations". Geotechnical Testing Journal, Vol.35
34. Richter, C., (2006). "Seasonal Variations in the Moduli of Unbound Pavement Layers," Publication No. FHWA-HRT-04-079, Turner–Fairbanks Highway Research Center, McLean, Va.
35. Sabnis, A., Abdallah, I., Pacheco, L. Nazarian, S., and Puppala, A.J., (2009), "Impact of Moisture Variation on Strength and Deformation of Clays,"

Research Report No. 0-5430-01, Center for Transportation Infrastructure Systems, The University of Texas at El Paso, El Paso, Texas.

36. Santha, B.L., (1994) "Resilient Modulus of Subgrade Soils: Comparison of Two Constitutive Equations," Transportation Research Record 1462, Transportation Research Board, National Research Council, Washington, D.C., pp. 79–90.
37. Sawangsuriya, A., Edil, T. B., and Bosscher, P. J. (2008), "Modulus-suction-moisture relationship for compacted soils." National Research Council, Can.Geotech. J. Vol. 45.
38. Seim, D. K., (1989). "A Comprehensive Study on the Resilient Modulus of Subgrade Soils." Oregon State University, Corvallis, Oregon.
39. Siekmeier J. A., (2011). "Unsaturated Soil Mechanics Implementation during Pavement Construction Quality Assurance," proceedings of 59th Annual Geotechnical Engineering Conference, St. Paul, MN.
40. Thom, N. H., and Brown, S. F., (1988). "The effect of grading and density on the mechanical properties of a crushed dolomitic limestone." Proc., 14th ARRB Conf., Part 7, 94–100.
41. Titus-Glover, L., and Fernando, E.B., (1995). "Evaluation of Pavement Subgrade Material Properties and Test Procedures," Report No. FHWA/TX-96/1335-2, Texas Transportation Institute, Texas A&M University, College Station. TX.

42. Thudi, H. R., (2006). "Assessment of soil-water retention properties of lime and cement treated clays", Thesis submitted to the the department of civil engineering, The University of Texas at Arlington, Texas in partial fulfillment of the master degree.
43. Uzan, J., (1985). "Characterization of Granular Materials," Transportation Research Record 1022, Transportation Research Board, National Research Council, Washington DC., pp. 52-59.
44. Von Quintus, H. L. Rao., and Killingsworth, B., (1998). "Analyses Relating to Pavement Material Characterizations and Their Effects on Pavement Performance," FHWA-RD-97-085, Federal Highway Administration, McLean, Va.
45. VonQuintus, H.L., Rao, C., Bhattacharya, B., Titi, H., and English, R., (2010). "Evaluation of Intelligetn compaction technology for Densification of Roadway Subgrades and Structural Layers," Submitted to the Wisconsin Highway Research Program (WHRP), Draft Final Report.
46. Wolfe, W. E., and Butalia, T. S., (2004). "Seasonal Instrumentation of SHRP Pavements," Final Report for Ohio Department of Trasnportation, Ohio State University, Columbus.
47. Yau, A., and Von Quintus, H. L., (2002). "Study of LTPP Laboratory Resilient Modulus Test Data and Response Characteristics," Report No. FHWA-RD-02-051, Federal Highway Administration, McLean, Va.

48. Zaman, M., and Khoury, N., (2007). "Effect of Soil Suction and Moisture on Resilient Modulus of Subgrade Soils in Oklahoma," Final Report for Oklahoma Department of Transportation. Norman. Oklahoma.
49. Zapata, C.E., (2009). "Consideration of Climate in New AASHTO Mechanistic-Empirical Pavement Design Guide," Transportation Research Board Annual Meeting CD, Paper #09-2254.
50. Zapata, C.E., and Houston, W.N., (2008). "Calibration and Validation of the Enhanced Integrated Climatic Model for Pavement Design," NCHRP Report 602, National Cooperative Highway Research Program, Transportation Research Board, of the National Academies, Washington, DC., pp. 62.

BIOGRAPHICAL INFORMATION

Ranjan Kumar Rout was born on 22nd August 1988 in Vijayawada, Andhra Pradesh India. He completed his schooling and intermediate from Mother Teresa High School and Nalanda Junior College in 2003 and 2005 respectively and joined Bapatla Engineering College to pursue his bachelor's degree. He received his bachelor's degree in Civil engineering from Acharya Nagarjuna University in 2009. He joined the University of Texas at Arlington in 2010 to pursue his Masters in Civil Engineering with a major concentration in Geotechnical Engineering. During the course of his study the author worked as a graduate research assistant under Dr. Anand J. Puppala and had a chance to work in various research projects.